

# Vital-Rate Feedback and Threshold Harvesting in Size-Structured Populations

Louis Shuo Wang

<sup>2</sup>Department of Mathematics, Northeastern University, Boston, MA,  
02115, USA .

Contributing authors: [wang.s41@northeastern.edu](mailto:wang.s41@northeastern.edu);

## Abstract

Size-selective harvesting is often justified by the intuition that larger individuals have higher value and should therefore be harvested above a critical size. We study a controlled size-structured transport model in which a scalar environmental variable, generated by the population itself, modifies the vital rates  $g(\mathbf{E}, l)$  and  $\mu(\mathbf{E}, l)$ . The first result is a corrected stationary closure theory: crowding-suppressed growth increases residence density at the inflow, so the closure derivative is not determined by pointwise profile monotonicity. Instead,  $\Phi'(\mathbf{E}) = \mathbf{A}(\mathbf{E}) - \mathbf{C}(\mathbf{E})$ , an integrated balance between residence-time amplification and cumulative survival loss. The second result is an exact stationary adjoint reduction. The nonlocal switching correction has rank one,  $\mathbf{S} = \mathbf{S}_{\text{red}} - \frac{\mathbf{A}}{1-B}\psi$ , and its zero-discount feedback gain satisfies the identity  $\mathbf{B}(\mathbf{0}) = \Phi'(\mathbf{E}^*)$ . Thus the same scalar governs stationary closure sensitivity and threshold fragility. We also establish finite-horizon well-posedness and compactified optimal-control existence in a spatial- $\mathbf{BV}$  policy class. Numerical certification in a density-dependent von Bertalanffy model shows when minimum-size harvesting persists and when vital-rate feedback creates multiple-switch harvest windows.

**Keywords:** Size-structured populations; selective harvesting; environmental feedback; nonlocal adjoint; threshold policies.

**MSC Classification:** 92D25 , 35F46 , 49J20 , 49K20 , 35Q92

# 1 Introduction

## 1.1 Existing theory: structured populations and selective harvesting

Individual size governs growth, survival, reproductive output, susceptibility to harvesting gear, and economic value. Population models that retain size as a continuous physiological coordinate are therefore a natural framework for selective harvesting. In such models, the population density is transported through size by individual growth, depleted by natural and harvesting mortality, and replenished through an inflow or renewal boundary. The resulting dynamics belong to the general theory of physiologically structured populations [1–8].

A central feature of this theory is the environmental interaction variable: individuals alter a finite-dimensional environmental quantity, while that quantity modifies their vital rates. At steady state, the problem separates into an individual-level balance under a frozen environment and a population-level consistency condition that closes the feedback loop [2]. For a scalar environment  $E$ , this frequently leads to a closure equation of the form  $E = \Phi(E)$ . Scalar reductions, their monotonicity properties, and their relation to persistence are classical [1, 4, 9–13]. The corresponding linearization around a steady state is also known to have finite-dimensional feedback structure in the environmental coordinate, with characteristic equations obtained from scalar or finite-dimensional closure loops [2, 14–16]. Thus the use of an aggregate crowding variable, the reduction of a stationary structured model to a scalar consistency equation, and the finite-rank character of the environmental feedback linearization form part of the established structured-population framework.

Optimal harvesting of continuously structured populations is likewise a mature subject, with deep roots in fisheries bioeconomics [17–19]. Early work on age-structured harvesting established optimality conditions and characteristic-based control formulations for McKendrick–von Foerster equations [20–27]. For size-structured populations, Kato proved existence of an optimal harvesting rate for a nonlinear model with separable mortality and nonlinear fertility, and separately derived a maximum principle and sufficient bang–bang conditions for a linear size-structured model [28, 29]. Hritonenko, Yatsenko, Goetz and Xabadia established maximum-principle and bang–bang results for age- and size-structured harvesting models, including size-structured forest management [30]. Davydov and Platov studied stationary profit maximization when growth, mortality, and exploitation depend on size alone, obtaining existence, uniqueness, and necessary optimality conditions under explicit parameter assumptions [31].

Subsequent work has broadened the theory to include size-dependent areas of action, spatial structure, discontinuous controls, hierarchical competition, nonlocal boundary feedback, impulse controls, and measure-valued controls [11, 32–38]. Measure-valued and balance-law formulations provide compactness frameworks when classical controls or densities develop concentrations or rapid oscillations [36, 39–43]. Recent studies continue this line by considering density dependence, arbitrary length-dependent harvest schedules, generic cost functionals, and alternative optimal-control

formulations [19, 44]; broader optimal-control theory for age-structured dynamic models provides further context [45–50]. In particular, Kakumani and Tumuluri [44] treat optimal harvesting for a nonlinear McKendrick–von Foerster equation with a generic cost functional.

The closest work to the present application is that of Opmeer [19], which permits an arbitrary length-dependent harvesting schedule in a density-dependent age/length formulation and numerically finds a conventional minimum-size optimum. The present paper differs in its analytical focus. Here the environmental feedback enters directly through the size-transport vital rates  $g(E, l)$  and  $\mu(E, l)$ , rather than only through recruitment, boundary feedback, or a size-only exploitation term. This changes both the stationary closure and the harvesting switching function. First, density-suppressed growth increases the residence density at the inflow, so the sign of the stationary closure derivative cannot be inferred from pointwise profile monotonicity; it is determined by an integrated balance of residence-time amplification and cumulative survival loss. Second, the stationary adjoint receives a full nonlocal correction that reduces exactly to a rank-one term. Its zero-discount gain is the stationary closure derivative,  $B|_{r=0} = \Phi'(E^*)$ .

The paper therefore has two main analytical contributions and three supporting components. The main contributions are: (i) a corrected stationary closure criterion showing why vital-rate feedback destroys pointwise monotonicity but can still yield an integrated uniqueness certificate; and (ii) an exact rank-one stationary switching correction, together with the identity  $B|_{r=0} = \Phi'(E^*)$ , which links closure sensitivity and adjoint feedback gain. The supporting components are: (iii) finite-horizon well-posedness in a spatial- $BV$  policy class; (iv) compactified optimal-control existence for bounded-complexity size-selective policies; and (v) numerical certification in a density-dependent von Bertalanffy model, including regimes where a conventional minimum-size rule persists and regimes where it fails.

## 1.2 Model and point of departure

Let

$$\Omega = [l_0, l_m], \quad 0 < l_0 < l_m < \infty,$$

be a bounded physiological-size domain. The population density  $x = x(t, l) \geq 0$  satisfies the controlled transport equation [6, 51]

$$\partial_t x + \partial_l(g(E(t), l)x) = -(\mu(E(t), l) + u(t, l))x, \quad E(t) = \int_{l_0}^{l_m} \chi(l)x(t, l) dl, \quad (1)$$

with initial datum  $x(0, \cdot) = \phi$  and prescribed inflow flux  $g(E(t), l_0)x(t, l_0) = p(t)$ . Here  $g(E, l) > 0$  is the somatic growth rate,  $\mu(E, l) \geq 0$  is natural mortality,  $u(t, l)$  is size-specific harvesting mortality, and  $E(t)$  is a weighted crowding or resource-pressure variable. Depending on the weight  $\chi$ , the environment may represent abundance, biomass, metabolic demand, or a more general load. We assume the compensatory signs

$$\partial_E g(E, l) \leq 0, \quad \partial_E \mu(E, l) \geq 0, \quad (2)$$

so that crowding slows growth and increases mortality.

The harvesting control satisfies  $0 \leq u(t, l) \leq u_{\max}$  a.e. on  $(0, T) \times \Omega$ , and the finite-horizon discounted yield is

$$J_T(u) = \int_0^T e^{-rt} \int_{l_0}^{l_m} c(l)u(t, l)x(t, l) dl dt, \quad r > 0. \quad (3)$$

Because the payoff is affine in  $u$ , a maximum-principle argument naturally leads to bang–bang harvesting. The central structural question is stronger: when is the bang–bang law also a minimum-size policy,  $u(t, l) = u_{\max} \mathbf{1}_{\{l > L(t)\}}$ ? A bang–bang law only asserts that  $u^*(t, l) \in \{0, u_{\max}\}$  a.e.; a minimum-size law additionally requires the harvested set to be an upper interval in size. If the switching function is  $S(t, l) = c(l) - \lambda(t, l)$ , then bang–bang control follows from the sign of  $S$ , whereas a threshold policy requires an upward single crossing of  $S(t, \cdot)$ . Global monotonicity of  $S(t, \cdot)$  is sufficient, but not necessary, for this property.

The environmental feedback in (1) changes the stationary closure in a simple but important way. For a stationary environment  $E$  and stationary control  $u = u(l)$ , the frozen- $E$  profile is

$$x_E(l) = \frac{p}{g(E, l)} \exp\left(-\int_{l_0}^l \frac{\mu(E, \xi) + u(\xi)}{g(E, \xi)} d\xi\right),$$

and stationarity requires the scalar consistency condition

$$E = \Phi(E), \quad \Phi(E) := \int_{l_0}^{l_m} \chi(l)x_E(l) dl.$$

Although (2) suggests that crowding should lower the profile, pointwise monotonicity fails at the inflow. If  $\chi(l_0) > 0$ , then

$$\partial_E \log(\chi(l_0)x_E(l_0)) = -\frac{\partial_E g(E, l_0)}{g(E, l_0)} \geq 0,$$

with strict inequality whenever growth is genuinely suppressed at  $l_0$ . The reason is that the boundary prescribes entering flux, not entering density: slower growth raises the residence density  $p/g(E, l_0)$  of newly entering individuals. Farther along the size domain, increased mortality and delayed progression reduce survival. Hence the derivative of the closure map is governed by an integrated balance  $\Phi'(E) = A(E) - C(E)$ , where  $A(E)$  is residence-time amplification and  $C(E)$  is cumulative survival/progression loss. This balance, rather than a pointwise sign condition on  $\partial_E x_E$ , is the relevant stationary uniqueness criterion.

The same vital-rate feedback also produces a nonlocal adjoint correction. Since

$$\delta E(t) = \int_{l_0}^{l_m} \chi(\xi) \delta x(t, \xi) d\xi,$$

variations of  $g(E, l)$  and  $\mu(E, l)$  generate the formal source

$$\chi(l) \int_{l_0}^{l_m} \left( \partial_E g(E, \xi) \partial_\xi \lambda(\xi) - \partial_E \mu(E, \xi) \lambda(\xi) \right) x(\xi) d\xi. \quad (4)$$

This is the mechanism absent from size-only adjoints or from models in which feedback enters only through a recruitment or boundary functional. In the spatial- $BV$  setting appropriate for finite-switch bang–bang policies, the term involving  $\partial_\xi \lambda$  must be interpreted by a  $BV$  integration-by-parts identity, which converts (4) into a bounded zeroth-order nonlocal functional of the costate.

In the stationary canonical problem this nonlocality admits an exact scalar reduction. Let  $\lambda_{\text{red}}$  be the reduced adjoint obtained by freezing the environment and omitting the nonlocal sensitivity term, and let  $\psi$  be the response to one unit of scalar environmental source. Then the full stationary adjoint has the form

$$\lambda = \lambda_{\text{red}} + \Gamma \psi, \quad \Gamma = \frac{A}{1 - B},$$

where  $A$  and  $B$  are explicit scalar integrals at the operating point. Hence

$$S = S_{\text{red}} - \Gamma \psi, \quad S_{\text{red}} := c - \lambda_{\text{red}}.$$

The threshold question is thereby reduced to the sign geometry of a computable rank-one correction. The main stationary identity proved below is  $B|_{r=0} = \Phi'(E^*)$ , so the zero-discount adjoint feedback gain is exactly the stationary closure derivative. This identity is the link between the corrected closure criterion and the preservation or failure of minimum-size harvesting.

### 1.3 Main contributions

The paper has two main analytical contributions and three supporting components. The first main contribution is a corrected stationary closure criterion for size-structured populations whose environmental feedback enters the vital rates  $g(E, l)$  and  $\mu(E, l)$ . We show that density-suppressed growth raises the residence density at the inflow, so pointwise profile monotonicity fails; uniqueness is instead governed by the integrated balance  $\Phi'(E) = A(E) - C(E)$ . The second main contribution is an exact rank-one reduction of the stationary nonlocal adjoint:

$$\lambda = \lambda_{\text{red}} + \frac{A}{1 - B} \psi, \quad S = S_{\text{red}} - \frac{A}{1 - B} \psi,$$

together with the identity  $B(0) = \Phi'(E^*)$ . Thus the zero-discount adjoint feedback gain is precisely the stationary closure derivative.

The supporting contributions are: finite-horizon well-posedness in a spatial- $BV$  policy class; compactified optimal-control existence for bounded-complexity size-selective harvesting policies; and numerical certification in a density-dependent von

Bertalanffy model, showing when minimum-size harvesting is preserved and when vital-rate feedback produces multiple-switch harvest windows.

## 1.4 Organization of the paper

Section 2 introduces the controlled size-structured model, the environmental feedback variable, and the harvesting objective. Section 3 derives the stationary closure equation  $E = \Phi(E)$  and the corrected integrated monotonicity criterion for uniqueness. Section 4 proves finite-horizon well-posedness in the spatial- $BV$  policy class. Section 5 separates forced persistence under prescribed recruitment from intrinsic demographic replacement. Section 6 establishes compactified optimal-control existence. Section 7 derives the nonlocal adjoint and the corresponding variational inequality, and Section 8 explains when bang–bang harvesting becomes a minimum-size policy. Section 9 contains the main stationary switching result: the exact rank-one correction and the identity  $B|_{r=0} = \Phi'(E^*)$ . Section 10 illustrates the theory in a density-dependent von Bertalanffy model and maps the regimes in which minimum-size harvesting persists or fails. Finally, Appendix provides detailed proofs for the mathematical conclusions in the main text.

## 2 Model and environmental feedback

### 2.1 Population state and physiological-size domain

For each  $t \geq 0$ , the state  $x(t, \cdot) \in L^1_+(\Omega)$  is the population-size density, so that  $\int_a^b x(t, l) dl$  is the number of individuals whose sizes lie in  $(a, b) \subseteq \Omega$ . In particular,  $N(t) := \int_{l_0}^{l_m} x(t, l) dl$  is total abundance. The lower endpoint  $l_0$  is the recruitment size; the upper endpoint  $l_m$  is an exit size. Because growth is strictly positive,  $l_0$  is an inflow boundary and  $l_m$  an outflow boundary. The model retains size but not age: individuals of the same current size share the same instantaneous rates at a given environmental state.

### 2.2 Environmental interaction variable

Density dependence is mediated by the scalar environmental interaction variable

$$E(t) := \int_{l_0}^{l_m} \chi(l)x(t, l) dl, \quad \chi \in L^{\infty}_+(\Omega). \quad (5)$$

Since  $0 \leq E(t) \leq \|\chi\|_{L^{\infty}(\Omega)}N(t)$ , the environment is controlled by total abundance but need not coincide with it. The functional (5) is the finite-dimensional environmental closure of the structured model [1, 2], separating the population–environment interaction into a readout  $x \mapsto E = \int_{\Omega} \chi x dl$  and a feedback  $E \mapsto (g(E, \cdot), \mu(E, \cdot))$ . Different choices of  $\chi$  encode different mechanisms:  $\chi \equiv 1$  gives  $E = N$ ;  $\chi(l) = l$  gives a length-weighted load;  $\chi(l) = \alpha l^{\beta}$  approximates a biomass or metabolic-demand load.

The scalar closure is deliberately parsimonious: it represents competition for a shared limiting resource without an explicit resource equation, on the assumption that the relevant environmental response is fast or well summarized by  $E[x]$ .

### 2.3 Growth and natural mortality

Let  $g : \mathbb{R}_+ \times \Omega \rightarrow \mathbb{R}_+$  and  $\mu : \mathbb{R}_+ \times \Omega \rightarrow \mathbb{R}_+$  be the growth and mortality rates. We assume

$$g, \mu \in C^1(\mathbb{R}_+ \times \Omega), \quad (6)$$

$$\text{for every } M > 0 : \quad 0 < g_{\min}(M) \leq g(E, l) \leq g_{\max}(M) < \infty \quad \text{on } [0, M] \times \Omega, \quad (7)$$

$$\mu(E, l) \geq \mu_{\min} \geq 0, \quad (8)$$

$$\partial_E g(E, l) \leq 0, \quad \partial_E \mu(E, l) \geq 0, \quad (9)$$

$$\partial_E g, \partial_l g, \partial_E \mu, \partial_l \mu \text{ are locally bounded on } \mathbb{R}_+ \times \Omega. \quad (10)$$

Assumption (7) is the bounded-environment positivity bound: on each bounded environmental interval  $[0, M]$  growth is strictly positive, so characteristics move from  $l_0$  toward  $l_m$  and no boundary condition is needed at  $l_m$ . We use it on the invariant interval  $[0, M_T]$  in the finite-horizon analysis (Section 4) and on a stationary closure interval  $[0, M_{\text{st}}]$  in Section 3; the calibrated growth law of Section 10 satisfies (7) in this local form (its infimum over all  $E \geq 0$  is zero, but it is bounded below on every  $[0, M]$ ). The signs (9) describe compensatory density dependence. Slower growth increases residence time within a size interval, which can locally increase  $x(t, l)$ ; increased mortality decreases survival to larger sizes. The competition between residence-time accumulation and mortality loss is the source of the corrected integrated closure analysis of Section 3.

As shown in Figure 1, the critical characteristic (dashed line) partitions the phase plane into the initial-datum-fed region and the boundary-flux-fed region. The typical flattening of the curves near  $l_0$  directly reflects the mathematical profile of the growth rate  $g(E, l)$ .

### 2.4 Size-selective harvesting

The control  $u = u(t, l)$  is the instantaneous fishing mortality, with the box constraint

$$0 \leq u(t, l) \leq u_{\max} \quad \text{for a.e. } (t, l) \in (0, T) \times \Omega,$$

and the admissible  $L^\infty$  class is

$$\mathcal{U}_{ad} := \{u \in L^\infty((0, T) \times \Omega) : 0 \leq u \leq u_{\max} \text{ a.e.}\}.$$

A threshold or minimum-size policy is

$$u_L(t, l) = u_{\max} \mathbf{1}_{\{l > L(t)\}}, \quad L(t) \in [l_0, l_m]. \quad (11)$$

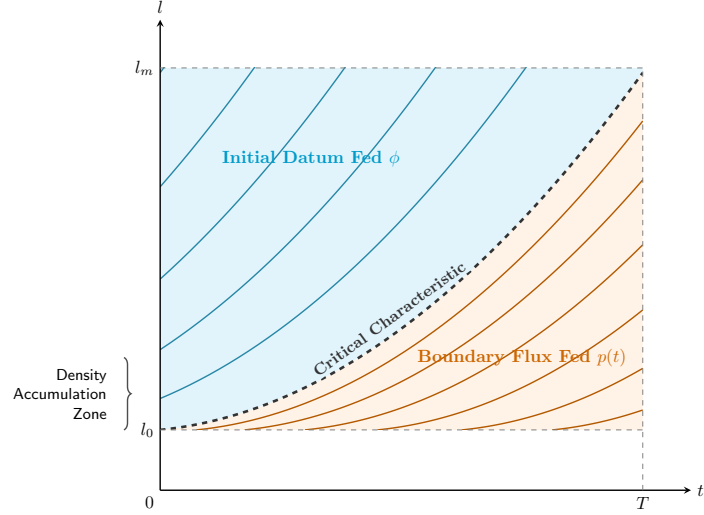


**Fig. 1** Typical shape of characteristic curves. The dashed critical characteristic separates the initial-datum-fed region (cyan) from the boundary-flux-fed region (orange), with its curvature determined by the growth rate  $g(E, l)$ .

Such regulations are common because they are observable, enforceable, and protect immature individuals [52, 53]; nevertheless (11) is only one possible size-selective policy. With  $c(l) \geq 0$  the value per harvested individual, the discounted yield is (3). Although  $c$  is often increasing in size, monotonicity of  $c$  alone does not imply a threshold policy, because the opportunity cost is the adjoint variable, which may itself depend non-monotonically on size.

## 2.5 Controlled population equation

The controlled dynamics are

$$\partial_t x + \partial_l (g(E(t), l)x) = -(\mu(E(t), l) + u(t, l))x, \quad (t, l) \in (0, T) \times \Omega, \quad (12)$$

with  $E(t) = \int_{l_0}^{l_m} \chi(l)x(t, l) dl$  and data

$$x(0, l) = \phi(l), \quad g(E(t), l_0)x(t, l_0) = p(t). \quad (13)$$

Expanding the flux gives the characteristic form

$$\partial_t x + g(E(t), l)\partial_l x = -(\partial_l g(E(t), l) + \mu(E(t), l) + u(t, l))x,$$

in which  $-\partial_l g x$  is the Jacobian compression/dilution term of nonuniform transport, not a demographic loss. The data satisfy

$$\phi \in L_+^1(\Omega) \cap L^\infty(\Omega), \quad p \in L_+^\infty(0, T), \quad \chi \in L_+^\infty(\Omega).$$

Additional  $BV$  assumptions are imposed only when needed in Sections 4 and 7.

## 2.6 Population balance and a priori estimate

Integrating (12) over  $\Omega$  and using the inflow condition,

$$\begin{aligned} N'(t) &= p(t) - g(E(t), l_m)x(t, l_m) - \int_{l_0}^{l_m} (\mu(E(t), l) + u(t, l))x(t, l) dl \\ &\leq p(t) - \mu_{\min}N(t), \end{aligned} \quad (14)$$

so that

$$N(t) \leq e^{-\mu_{\min}t}N(0) + \int_0^t e^{-\mu_{\min}(t-s)}p(s) ds \quad (\mu_{\min} > 0),$$

with the obvious modification when  $\mu_{\min} = 0$ . Consequently

$$0 \leq E(t) \leq \|\chi\|_{L^\infty(\Omega)}N(t) \leq M_T, \quad (15)$$

for a constant  $M_T$  depending on the horizon and data but not on the particular admissible control. This confines all coefficient evaluations to the compact environmental interval  $[0, M_T]$ .

The non-linear coupling of the system is illustrated in Figure 2. The feedback loop is closed as the population density determines the environmental index  $E(t)$ , which in turn modulates the vital rates.

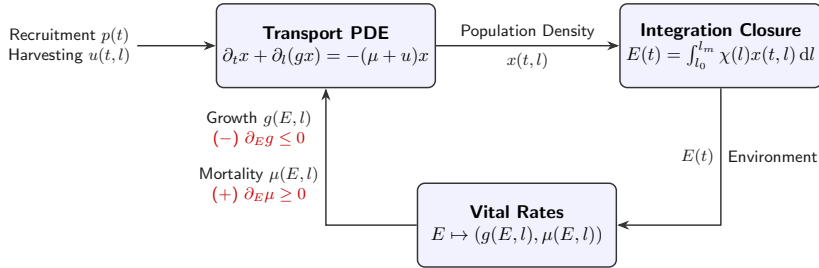


**Fig. 2** Feedback loop of the size-structured model. The population density couples with the integration closure via the environment-dependent vital rates  $(g, \mu)$ .

## 2.7 Exogenous recruitment and scope

The inflow  $p(t)$  is prescribed independently of the population, so the model describes exogenous recruitment. If  $p(t) > 0$ , the population may persist even when its own

reproductive output is insufficient to replace harvested individuals; positivity of the forced system must not be read as demographic self-sustainability. The endogenous counterpart replaces (13) by a renewal boundary condition; this diagnostic is developed in Section 5. The optimization problem studied here is the forced problem (12)–(13).

### 3 Stationary closure and failure of pointwise monotonicity

Throughout this section assume

$$p(t) \equiv p > 0, \quad u(t, l) \equiv u(l) \in L^\infty(\Omega), \quad 0 \leq u(l) \leq u_{\max} \text{ a.e.}, \quad (16)$$

together with (6)–(10) and bounded continuous  $E$ -derivatives on every compact environmental interval, justifying differentiation under the integral sign.

#### 3.1 Frozen-environment stationary profile

A stationary pair  $(x, E)$  satisfies

$$\frac{d}{dl}(g(E, l)x(l)) = -(\mu(E, l) + u(l))x(l), \quad g(E, l_0)x(l_0) = p, \quad E = \int_{l_0}^{l_m} \chi(l)x(l) dl.$$

With the mortality-to-growth ratio

$$q(E, l) := \frac{\mu(E, l) + u(l)}{g(E, l)} \geq 0$$

and  $y_E := g(E, \cdot)x_E$  solving  $y'_E = -q(E, \cdot)y_E$ ,  $y_E(l_0) = p$ , one obtains

$$x_E(l) = \frac{p}{g(E, l)} \exp\left(-\int_{l_0}^l \frac{\mu(E, \xi) + u(\xi)}{g(E, \xi)} d\xi\right) = p \frac{1}{g(E, l)} \sigma_E(l), \quad (17)$$

where  $\sigma_E(l) = \exp(-\int_{l_0}^l q)$  is the survival to size  $l$  and  $1/g(E, l)$  the residence time per unit size.

**Proposition 3.1** (Frozen-environment profile). *For every  $E \in [0, M_{\text{st}}]$  and every  $u$  as in (16), the stationary transport equation with flux datum  $p$  has the unique solution (17), and  $0 < x_E(l) \leq p/g_{\min}(M_{\text{st}})$  on  $\Omega$ .*

#### 3.2 Scalar environmental closure

Define the closure map

$$\Phi(E) := \int_{l_0}^{l_m} \chi(l)x_E(l) dl, \quad (18)$$

so that the stationary consistency condition is  $E = \Phi(E)$ .

**Proposition 3.2** (Existence of a stationary environment). *With  $g_{\min}(M) := \inf_{[0, M] \times \Omega} g > 0$  from (7),*

$$0 \leq \Phi(E) \leq \frac{p \|\chi\|_{L^\infty(\Omega)}}{g_{\min}(M)} (l_m - l_0) =: G(M) \quad \text{for } E \in [0, M]. \quad (19)$$

*Assume the closure-confinement condition*

$$\exists M_{\text{st}} > 0 : \quad \Phi([0, M_{\text{st}}]) \subseteq [0, M_{\text{st}}]. \quad (\text{H-st})$$

*Then  $\Phi$  is continuous on  $[0, M_{\text{st}}]$  and  $E = \Phi(E)$  has at least one fixed point  $E^* \in [0, M_{\text{st}}]$ . If  $\chi \geq 0$  is positive on a set of positive measure, then  $\Phi(E) > 0$  and every fixed point is positive.*

*Remark 3.3* (On (H-st) and how it is met). Condition (H-st) is a genuine restriction, not automatic. Two sufficient conditions are useful. (a) *Crude a priori bound.* If  $G(M_{\text{st}}) \leq M_{\text{st}}$  for some  $M_{\text{st}}$ , then (H-st) holds; but  $G$  may fail this for all  $M$ , since  $g_{\min}(M)$  can decay so fast that  $G$  grows faster than  $M$  (e.g.  $g_{\min}(M) \sim (1+M)^{-2}$  gives  $G(M) \sim (1+M)^2$ ). This crude test is often far too conservative because (19) discards survival and the weighting. (b) *Decreasing closure map.* If  $\Phi$  is nonincreasing on  $[0, \infty)$ , then  $M_{\text{st}} := \Phi(0)$  satisfies (H-st), since  $0 \leq \Phi(E) \leq \Phi(0)$  for  $E \in [0, \Phi(0)]$ . For the calibrated von Bertalanffy model of Section 10 the crude test (a) does not hold at the baseline (the bound  $G$  overestimates  $\Phi$  by orders of magnitude), but  $\Phi$  is decreasing on the relevant range (Figure 5), so (b) applies and we use  $M_{\text{st}} = \Phi(0) \approx 1.04$ ; this is the interval on which the numerical closure diagnostics are evaluated. Monotonicity of  $\Phi$  also yields uniqueness (Theorem 3.7); where  $\Phi$  is not globally monotone, (H-st) must be checked directly, as we do numerically.

*Remark 3.4* (Relation to existing theory). Environmental closure equations and their fixed points are classical [1, 2, 4], and stationary size-only exploitation has been studied [31]. We claim no novelty for (18) or Proposition 3.2. The point of this section is that feedback through the rates makes the sign of  $\Phi'(E)$  a competition of two integrated effects, so monotonicity cannot be read off from  $\partial_E g \leq 0$ ,  $\partial_E \mu \geq 0$  pointwise.

### 3.3 Sensitivity of the frozen profile

To avoid the symbol clash with the discounted-mortality coefficient introduced in Section 9, we write the growth-sensitivity coefficient here as  $\alpha$ :

$$\alpha(E, l) := -\frac{\partial_E g(E, l)}{g(E, l)}, \quad b(E, l) := \partial_E q(E, l) = \partial_E \left( \frac{\mu(E, l) + u(l)}{g(E, l)} \right). \quad (20)$$

Under (9),  $\alpha(E, l) \geq 0$  and

$$b(E, l) = \frac{\partial_E \mu(E, l) g(E, l) - (\mu(E, l) + u(l)) \partial_E g(E, l)}{g(E, l)^2} \geq 0, \quad (21)$$

the latter a sum of two nonnegative terms. The logarithmic derivative of (17) is

$$\partial_E \log x_E(l) = \alpha(E, l) - \int_{l_0}^l b(E, \xi) d\xi, \quad \partial_E x_E(l) = x_E(l) \left[ \alpha(E, l) - \int_{l_0}^l b(E, \xi) d\xi \right]. \quad (22)$$

Thus the sensitivity is a positive local residence-time term  $\alpha$  minus a negative cumulative survival/progression term.

### 3.4 Failure of pointwise monotonicity at the inflow

A naive sufficient condition for strict decrease of  $\Phi$  is  $\partial_E x_E(l) < 0$  for all  $l$ , i.e.  $\alpha(E, l) < \int_{l_0}^l b(E, \xi) d\xi$  for all  $l$ . This is incompatible with the inflow structure.

**Proposition 3.5** (Pointwise monotonicity fails at the inflow). *For every  $E \geq 0$ ,*

$$x_E(l_0) = \frac{p}{g(E, l_0)}, \quad \partial_E x_E(l_0) = -\frac{p \partial_E g(E, l_0)}{g(E, l_0)^2} = x_E(l_0) \alpha(E, l_0) \geq 0. \quad (23)$$

*If  $\partial_E g(E, l_0) < 0$ , then  $\partial_E x_E(l_0) > 0$ , and by continuity there is  $\delta_E > 0$  with  $\partial_E x_E(l) > 0$  for  $l \in [l_0, l_0 + \delta_E)$ . Hence the pointwise decreasing-profile condition cannot hold whenever growth is strictly crowding-suppressed at the inflow.*

*Remark 3.6* (Ecological reading). The boundary prescribes the entering flux  $p$ , not the entering density. Since  $x_E(l_0) = p/g(E, l_0)$ , slower growth keeps recruits longer near  $l_0$  and raises their density there, before any cumulative mortality acts.

Differentiating (18) under the integral sign and using (22),

$$\Phi'(E) = \int_{l_0}^{l_m} \chi(l) x_E(l) \left[ \alpha(E, l) - \int_{l_0}^l b(E, \xi) d\xi \right] dl.$$

With the tail load  $W_E(\xi) := \int_{\xi}^{l_m} \chi(l) x_E(l) dl$ , Fubini's theorem gives

$$\Phi'(E) = \underbrace{\int_{l_0}^{l_m} \chi(l) x_E(l) \alpha(E, l) dl}_{A(E)} - \underbrace{\int_{l_0}^{l_m} b(E, \xi) W_E(\xi) d\xi}_{C(E)}. \quad (24)$$

Here  $A(E) \geq 0$  is the residence-time amplification induced by crowding-suppressed growth, while  $C(E) \geq 0$  is the cumulative survival/progression loss, weighted by the downstream tail load  $W_E$ .

**Theorem 3.7** (Integrated monotonicity: a sufficient uniqueness certificate). *If*

$$C(E) > A(E) \quad \text{for every } E \in [0, M_{\text{st}}],$$

equivalently  $\Phi'(E) < 0$  on  $[0, M_{\text{st}}]$ , then  $\Phi$  is strictly decreasing on  $[0, M_{\text{st}}]$ , and  $E = \Phi(E)$  has exactly one solution  $E^* \in [0, M_{\text{st}}]$ , with unique profile  $x^* = x_{E^*}$ . This global integrated-monotonicity condition is sufficient for uniqueness; it is not necessary, since a non-monotone  $\Phi$  may still meet the identity once.

**Corollary 3.8** (Uniform margin). *If  $C(E) - A(E) \geq \kappa > 0$  on  $[0, M_{\text{st}}]$ , then  $\Phi'(E) \leq -\kappa$ , so the sufficient condition of Theorem 3.7 holds with a margin and is robust under perturbations preserving it.*

*Remark 3.9* (Why the integrated form is the appropriate test). Pointwise decrease would imply  $\Phi' < 0$ , but Proposition 3.5 shows it is unattainable at the inflow. The integrated condition (24) permits  $\partial_E x_E(l) > 0$  near  $l_0$  provided the weighted negative sensitivity at larger sizes dominates. It is thus not merely weaker than a pointwise test; it is the monotonicity-based sufficient uniqueness condition compatible with the model's inflow structure.

*Remark 3.10* (Forward pointer). The quantity  $\Phi'(E^*) = A - C$  reappears in Section 9 as the zero-discount value of the adjoint feedback gain: Theorem 9.11 shows  $B|_{r=0} = \Phi'(E^*)$ . The residence-time term  $A$  is, there, exactly the boundary leftover of the auxiliary backward equation, and  $C$  its forward/adjoint dual.

### 3.5 A computable closure certificate

For  $E \in [0, M_{\text{st}}]$ , define

$$\Delta_\Phi(E) := C(E) - A(E) = -\Phi'(E).$$

Then  $\Delta_\Phi(E) > 0$  is equivalent to  $\Phi'(E) < 0$ . A numerical check of  $\Delta_\Phi > 0$  on a grid is evidence for strict monotonicity; a rigorous certificate follows by enclosing the profile, quadratures, and interpolation error with interval arithmetic, or by combining grid values with an a posteriori bound on  $\sup_{[E_j, E_{j+1}]} |\Phi''|$ . The von Bertalanffy verification appears in Section 10.

## 4 Finite-horizon well-posedness

Existence, stability, and compactness for structured transport equations with nonlocal coefficients are available in measure-valued and Lagrangian frameworks [41, 54, 55]. Because the present model has a strictly positive  $C^1$  speed and bounded inflow, a direct characteristic argument suffices. We work in the spatial- $BV$ -compatible class

$$\mathcal{U}_T^{\text{WP}}(C_u) := \left\{ u \in L^\infty((0, T) \times \Omega) : 0 \leq u \leq u_{\max} \text{ a.e., } \operatorname{ess\,sup}_{t \in (0, T)} \operatorname{TV}_\Omega(u(t, \cdot)) \leq C_u \right\},$$

which contains the threshold controls and coincides with the admissible class of Section 6. Assume

$$\phi \in BV(\Omega) \cap L_+^\infty(\Omega), \quad p \in BV(0, T) \cap L_+^\infty(0, T), \quad \chi \in W_+^{1, \infty}(\Omega), \quad (25)$$

together with (6)–(10) and, on every  $[0, M]$ ,

$$\sup_{E \in [0, M]} \left( \|\partial_E g(E, \cdot)\|_{W^{1, \infty}(\Omega)} + \|\partial_E \mu(E, \cdot)\|_{L^\infty(\Omega)} + \|\partial_t g(E, \cdot)\|_{BV(\Omega)} + \|\mu(E, \cdot)\|_{BV(\Omega)} \right) < \infty. \quad (26)$$

#### 4.1 Weak formulation and population bound

**Definition 4.1** (Weak solution). For  $u \in \mathcal{U}_T^{\text{wp}}(C_u)$ , a nonnegative  $x \in C([0, T]; L^1(\Omega)) \cap L^\infty((0, T) \times \Omega)$  with  $E(t) = \int_\Omega \chi x(t, \cdot)$  is a weak solution if, for all  $\psi \in C^1([0, T] \times \Omega)$  with  $\psi(T, \cdot) = 0$  and  $\psi(\cdot, l_m) = 0$ ,

$$\int_0^T \int_\Omega x [\partial_t \psi + g(E, l) \partial_l \psi - (\mu(E, l) + u) \psi] \, dl \, dt + \int_\Omega \phi \psi(0, \cdot) \, dl + \int_0^T p \psi(\cdot, l_0) \, dt = 0.$$

The population balance (14) gives  $N' \leq p - \mu_{\min} N$ , hence  $N(t) \leq C_T^N$  and  $0 \leq E(t) \leq \|\chi\|_{L^\infty(\Omega)} C_T^N =: M_T$ , uniformly over  $\mathcal{U}_T^{\text{wp}}(C_u)$ .

For the time-modulus estimates of Section 6 and for the environmental-regularity bound below we record a Green identity for the characteristic solution. It is not a consequence of Definition 4.1 alone, whose test functions vanish at  $l_m$ ; it is proved directly from the representation (28).

**Lemma 4.2** (Outflow trace and Green identity). *Let  $x$  be the (frozen or coupled) characteristic solution with data (25). Then the outflow flux trace  $\beta(t) := g(E(t), l_m) x(t, l_m^-)$  is well defined for a.e.  $t$  and lies in  $L^\infty(0, T)$ , with  $\|\beta\|_{L^\infty} \leq g_{\max} C_T^0$ ,  $C_T^0$  the  $L^\infty$  state bound (29). Moreover, for every  $\psi \in W^{1, \infty}(\Omega)$  and  $0 \leq t \leq t+h \leq T$ ,*

$$\begin{aligned} \int_\Omega (x(t+h, \cdot) - x(t, \cdot)) \psi \, dl &= \int_t^{t+h} \int_\Omega \left( g(E, l) x \partial_l \psi - (\mu(E, l) + u) x \psi \right) \, dl \, ds \\ &\quad + \int_t^{t+h} p(s) \psi(l_0) \, ds - \int_t^{t+h} g(E(s), l_m) x(s, l_m^-) \psi(l_m) \, ds. \end{aligned} \quad (27)$$

#### 4.2 Frozen-environment problem

Let  $\mathcal{B}_{M_T} := \{E \in C([0, T]) : 0 \leq E \leq M_T\}$  and, for  $L_E > 0$ , the closed Lipschitz subclass

$$\mathcal{B}_{M_T}^{L_E} := \{E \in \mathcal{B}_{M_T} : |E(t) - E(s)| \leq L_E |t - s| \, \forall s, t\},$$

which is convex and closed in  $C([0, T])$  (a uniform limit of  $L_E$ -Lipschitz functions is  $L_E$ -Lipschitz). For  $E \in \mathcal{B}_{M_T}$  let  $\eta_E(s; t, l)$  solve  $\frac{d}{ds} \eta_E = g(E(s), \eta_E)$ ,  $\eta_E(t; t, l) = l$ . Since  $g \geq g_{\min}$ , each backward characteristic meets the initial line  $s = 0$  or the inflow  $l = l_0$  (entrance time  $\tau_E(t, l)$ ). With

$$\mathcal{A}_E(a, t; l) := \exp\left(-\int_a^t [\partial_t g + \mu + u](E(s), \eta_E(s; t, l)) \, ds\right),$$

the representation is

$$x_E(t, l) = \begin{cases} \phi(\eta_E(0; t, l)) \mathcal{A}_E(0, t; l), & \eta_E(0; t, l) > l_0, \\ \frac{p(\tau_E(t, l))}{g(E(\tau_E(t, l)), l_0)} \mathcal{A}_E(\tau_E(t, l), t; l), & \eta_E(0; t, l) \leq l_0. \end{cases} \quad (28)$$

**Lemma 4.3** (Frozen-environment solution: existence and amplitude bounds). *For every  $E \in \mathcal{B}_{M_T}$ ,  $u \in \mathcal{U}_T^{\text{WP}}(C_u)$ , the frozen problem has a unique nonnegative weak solution  $x_E \in C([0, T]; L^1(\Omega)) \cap L^\infty((0, T) \times \Omega)$  with*

$$\sup_{t \in [0, T]} (\|x_E(t, \cdot)\|_{L^1} + \|x_E(t, \cdot)\|_{L^\infty}) + \|g(E, l_m) x_E(\cdot, l_m^-)\|_{L^\infty(0, T)} \leq C_T^0, \quad (29)$$

$C_T^0$  independent of  $E \in \mathcal{B}_{M_T}$  (in particular, independent of any modulus of continuity of  $E$ ).

*Remark 4.4* (Why a  $BV$  bound needs more than  $E \in C$ ). The boundary-fed branch of (28) contains the factor  $p(\tau_E(t, l))/g(E(\tau_E(t, l)), l_0)$ . With  $p \in BV(0, T)$  but  $E$  merely continuous, the map  $t \mapsto 1/g(E(t), l_0)$  can have infinite total variation, so its composition with the (monotone) entrance-time map need not be of bounded spatial variation. A spatial- $BV$  bound for  $x_E$  therefore cannot hold uniformly over  $\mathcal{B}_{M_T}$ ; it requires the environmental path itself to be of bounded temporal variation. We obtain this through a uniform Lipschitz bound on the coupled environment, derived next, and then restrict the fixed point to  $\mathcal{B}_{M_T}^{L_E}$ .

**Lemma 4.5** (Environmental regularity: uniform Lipschitz bound). *Assume  $\chi \in W_+^{1, \infty}(\Omega)$ . For every  $E \in \mathcal{B}_{M_T}$  the map  $t \mapsto (\mathcal{F}E)(t) := \int_\Omega \chi(l) x_E(t, l) dl$  is Lipschitz, with*

$$(\mathcal{F}E)'(t) = \chi(l_0)p(t) - \chi(l_m)g(E(t), l_m)x_E(t, l_m^-) + \int_\Omega g(E, l)x_E \chi'(l) dl - \int_\Omega \chi(l)(\mu(E, l) + u)x_E dl \quad (30)$$

for a.e.  $t$ , and the explicit bound

$$\text{ess sup}_{t \in (0, T)} |(\mathcal{F}E)'(t)| \leq L_E^* := \|\chi\|_\infty \|p\|_\infty + \|\chi\|_\infty g_{\max} C_T^0 + (g_{\max} \|\chi'\|_\infty + \|\chi\|_\infty (\mu_{\max, T} + u_{\max})) C_T^0, \quad (31)$$

with  $C_T^0$  from (29) and  $\mu_{\max, T} := \sup_{(E, l) \in [0, M_T] \times \Omega} \mu(E, l) < \infty$  (finite by (6) on the compact set). The constant  $L_E^*$  is independent of  $E \in \mathcal{B}_{M_T}$ . In particular  $\mathcal{F}$  maps  $\mathcal{B}_{M_T}$  into  $\mathcal{B}_{M_T}^{L_E^*}$ .

We henceforth fix  $L_E := L_E^*$  and work in  $\mathcal{B}_{M_T}^{L_E}$ .

**Lemma 4.6** (Frozen-environment spatial BV bound under a Lipschitz environment). For every  $E \in \mathcal{B}_{M_T}^{L_E}$  and  $u \in \mathcal{U}_T^{\text{wp}}(C_u)$ ,

$$\sup_{t \in [0, T]} \text{TV}_\Omega(x_E(t, \cdot)) \leq C_T, \quad (32)$$

with  $C_T$  depending on the data, the coefficient bounds (26),  $C_u$ , and  $L_E$ , but not otherwise on  $E$ .

### 4.3 Stability in the environmental trajectory

**Lemma 4.7** (Short-time environmental stability). Let  $E_1, E_2 \in \mathcal{B}_{M_T}^{L_E}$  with frozen solutions  $x_{E_1}, x_{E_2}$  for the same data and control. There is  $C_T > 0$  independent of  $E_1, E_2$  with, for every  $\tau \in (0, T]$ ,

$$\sup_{t \in [0, \tau]} \|x_{E_1}(t, \cdot) - x_{E_2}(t, \cdot)\|_{L^1(\Omega)} \leq C_T \tau \|E_1 - E_2\|_{C([0, \tau])}. \quad (33)$$

### 4.4 Nonlinear fixed point

By Lemma 4.5,  $\mathcal{F}$  maps  $\mathcal{B}_{M_T}$  into the closed convex Lipschitz class  $\mathcal{B}_{M_T}^{L_E}$ ; in particular  $\mathcal{F} : \mathcal{B}_{M_T}^{L_E} \rightarrow \mathcal{B}_{M_T}^{L_E}$ . On  $\mathcal{B}_{M_T}^{L_E}$  the frozen states obey the uniform spatial-BV bound of Lemma 4.6, so Lemma 4.7 applies and gives

$$\|\mathcal{F}E_1 - \mathcal{F}E_2\|_{C([0, \tau])} \leq \|\chi\|_{L^\infty} C_T \tau \|E_1 - E_2\|_{C([0, \tau])},$$

a contraction on  $\mathcal{B}_{M_T}^{L_E}$  for small  $\tau$ .

**Theorem 4.8** (Finite-horizon well-posedness). Assume (6)–(10), (25) (in particular  $\chi \in W_+^{1, \infty}(\Omega)$ ), and (26). For every  $u \in \mathcal{U}_T^{\text{wp}}(C_u)$ , problem (12)–(13) has a unique nonnegative weak solution  $x^u \in C([0, T]; L^1(\Omega)) \cap L^\infty((0, T) \times \Omega)$  whose environment  $E^u(t) = \int_\Omega \chi x^u(t, \cdot)$  is  $L_E$ -Lipschitz, with

$$\sup_{t \in [0, T]} (\|x^u(t, \cdot)\|_{L^1} + \|x^u(t, \cdot)\|_{L^\infty} + \text{TV}_\Omega(x^u(t, \cdot))) \leq C_T,$$

$C_T$  depending on  $T$ , data, coefficient bounds, and  $C_u$ , not on the control.

**Proposition 4.9** (Continuous dependence). For data and controls  $(\phi_i, p_i, u_i)$ ,  $u_i \in \mathcal{U}_T^{\text{wp}}(C_u)$ ,

$$\sup_t \|x_1 - x_2\|_{L^1(\Omega)} \leq C_T (\|\phi_1 - \phi_2\|_{L^1} + \|p_1 - p_2\|_{L^1(0, T)} + \|u_1 - u_2\|_{L^1}), \quad (34)$$

with  $C_T$  uniform under common  $L^\infty$  and spatial-BV bounds.

*Remark 4.10* (Scope). The spatial-BV hypothesis controls compositions of  $u$  and the data with nearby flows; an  $L^\infty$  bound alone controls amplitude but not sensitivity to

spatial translation. We therefore do not claim strong continuous dependence uniformly over  $\mathcal{U}_{ad}$ . Broader (Lagrangian and measure-valued) formulations are possible [41, 54, 56] but are outside our scope.

## 5 Forced persistence and intrinsic replacement

The forced model has exogenous recruitment, so persistence under prescribed  $p$  is not demographic self-sustainability. To diagnose intrinsic replacement we introduce the endogenous renewal counterpart, used here only as a diagnostic; the optimization remains the forced problem.

### 5.1 Replacement functional and basic reproduction number

Replace the inflow datum in (13) by the size-specific fertility renewal condition

$$g(E(t), l_0)x(t, l_0) = \int_{l_0}^{l_m} m(l)x(t, l) dl, \quad m \in L_+^\infty(\Omega). \quad (35)$$

At a stationary environment  $E$  with frozen profile normalized to unit recruitment flux,  $\hat{x}_E(l) := x_E(l)/p$ , define the environment- and harvest-dependent replacement functional

$$A(E; u) := \int_{l_0}^{l_m} m(l)\hat{x}_E(l) dl = \int_{l_0}^{l_m} \frac{m(l)}{g(E, l)} \exp\left(-\int_{l_0}^l \frac{\mu(E, \xi) + u(\xi)}{g(E, \xi)} d\xi\right) dl,$$

the expected lifetime offspring of a recruit at environment  $E$  under harvesting  $u$ . The conventional basic reproduction number is the value at the extinction (invasion) environment,  $\mathcal{R}_0(u) := \mathcal{R}(0; u)$ , the expected lifetime offspring in an empty population, as obtained from the next-generation operator of structured-population theory [2, 11]; we reserve the symbol  $\mathcal{R}_0$  for this invasion quantity and do not call  $\mathcal{R}(E; u)$  a reproduction number.

**Proposition 5.1** (Stationary renewal state: generation balance and amplitude). *A nontrivial stationary renewal state has the form  $x = b\hat{x}_E$  with  $b > 0$ , and exists at environment  $E^\dagger > 0$  if and only if both the generation-balance condition and the environmental closure hold:*

$$\mathcal{R}(E^\dagger; u) = 1 \quad \text{and} \quad b = \frac{E^\dagger}{\int_{l_0}^{l_m} \chi(l)\hat{x}_{E^\dagger}(l) dl}. \quad (36)$$

*If  $\chi > 0$  on a set of positive measure, no positive stationary state exists at  $E = 0$ . Moreover, under (9), increasing  $u$  pointwise does not increase  $\mathcal{R}(\cdot; u)$ ; and if  $\mathcal{R}(\cdot; u)$  is strictly decreasing in  $E$  on  $[0, M]$  with  $\mathcal{R}(0; u) > 1 > \mathcal{R}(M; u)$ , then  $E^\dagger$  is unique.*

## 5.2 Equilibrium-adjusted spawning-potential ratio

For a reference unfished equilibrium environment  $E_0$  (set  $u \equiv 0$ ) and a fished equilibrium  $E^*$ , define the equilibrium-adjusted spawning-potential ratio

$$\text{SPR}_{\text{eq}} := \frac{\int_{l_0}^{l_m} m(l) \hat{x}_{E^*}(l) dl}{\int_{l_0}^{l_m} m(l) \hat{x}_{E_0}^0(l) dl} = \frac{\mathcal{R}(E^*; u)}{\mathcal{R}(E_0; 0)},$$

where  $\hat{x}_{E_0}^0$  is the unit-recruitment unfished profile. This is a defensible per-recruit ratio, but it compares the fished and unfished states at their respective equilibrium environments and is therefore not the classical fixed-vital-rate SPR: under compensatory density feedback the vital rates differ between numerator and denominator, so  $\text{SPR}_{\text{eq}}$  may behave differently from a conventional fixed-environment SPR (for instance, density release at low abundance can raise per-recruit output and partially offset harvesting). It is the quantity against which the forced-optimal harvesting policies of Sections 7–9 are compared in Section 10. We emphasize that  $\text{SPR}_{\text{eq}} < 1$  is compatible with forced persistence: prescribed recruitment can sustain a population whose intrinsic replacement is below unity.

## 6 Compact admissible class and optimal-control existence

The finite-horizon problem is

$$V_T := \sup_{u \in \mathcal{U}_{ad}} J_T(u), \quad J_T(u) = \int_0^T e^{-rt} \int_{\Omega} c(l) u(t, l) x^u(t, l) dl dt.$$

The box class  $\mathcal{U}_{ad}$  is weak-\* compact, but weak-\* convergence  $u_n \xrightarrow{*} u$  need not pass to the bilinear product  $u_n x^{u_n}$ , the obstruction being spatial oscillation. We therefore introduce a spatial- $BV$  restriction as an explicit compactification, designed to yield strong compactness of the states, not of the controls. Throughout assume the hypotheses of Theorem 4.8 and  $c \in L_+^\infty(\Omega)$ .

### 6.1 Spatial- $BV$ compactification

Fix  $C_u \geq u_{\max}$  and set

$$\mathcal{U}_{ad}^{BV} := \left\{ u \in \mathcal{U}_{ad} : \text{ess sup}_{t \in (0, T)} \text{TV}_{\Omega}(u(t, \cdot)) \leq C_u \right\}, \quad V_T^{BV} := \sup_{u \in \mathcal{U}_{ad}^{BV}} J_T(u).$$

Every threshold control  $u_L$  satisfies  $\text{TV}_{\Omega}(u_L(t, \cdot)) \leq u_{\max}$ , so all threshold policies lie in  $\mathcal{U}_{ad}^{BV}$ ; a bang–bang control with at most  $k$  spatial switches has variation at most

$ku_{\max}$ . The budget admits the distributional form

$$\left| \int_0^T \int_{\Omega} u \partial_t \varphi \, dl \, dt \right| \leq C_u \int_0^T \|\varphi(t, \cdot)\|_{L^\infty(\Omega)} \, dt, \quad \varphi \in C_c^1((0, T) \times \Omega). \quad (37)$$

**Lemma 6.1** (Weak-\* compactness of  $\mathcal{U}_{ad}^{BV}$ ).  $\mathcal{U}_{ad}^{BV}$  is convex and sequentially weak-\* compact in  $L^\infty((0, T) \times \Omega)$ .

*Remark 6.2* (What is compactified).  $\mathcal{U}_{ad}$  is already weak-\* compact; the role of  $\mathcal{U}_{ad}^{BV}$  is to give uniform spatial regularity of the states and thereby make the control-to-state map sequentially closed under weak-\* convergence of controls.

## 6.2 Uniform state compactness

By Theorem 4.8,

$$\sup_{u \in \mathcal{U}_{ad}^{BV}} \sup_{t \in [0, T]} (\|x^u(t, \cdot)\|_{L^1} + \|x^u(t, \cdot)\|_{L^\infty} + \text{TV}_\Omega(x^u(t, \cdot))) \leq C_T. \quad (38)$$

We use the negative norm dual to  $W^{1, \infty}$ , defined explicitly by

$$\|f\|_{\mathcal{W}^{-1,1}(\Omega)} := \sup \left\{ |\langle f, \psi \rangle| : \psi \in W^{1, \infty}(\Omega), \|\psi\|_{W^{1, \infty}(\Omega)} \leq 1 \right\}.$$

**Lemma 6.3** (Uniform weak time modulus). *There is  $C_T > 0$ , independent of  $u \in \mathcal{U}_{ad}^{BV}$ , with*

$$\|x^u(t+h, \cdot) - x^u(t, \cdot)\|_{\mathcal{W}^{-1,1}(\Omega)} \leq C_T h, \quad 0 \leq t \leq t+h \leq T. \quad (39)$$

Using the one-dimensional interpolation inequality

$$\|v\|_{L^1(\Omega)} \leq C_\Omega \|v\|_{\mathcal{W}^{-1,1}(\Omega)}^{1/2} (\|v\|_{L^1(\Omega)} + \text{TV}_\Omega(v))^{1/2}, \quad v \in BV(\Omega), \quad (40)$$

(obtained by extending  $v$  to  $\mathbb{R}$ , mollifying at scale  $\varepsilon$ , and optimizing  $\|v\|_{L^1} \leq C_\Omega(\varepsilon \text{TV}(v) + \varepsilon^{-1} \|v\|_{\mathcal{W}^{-1,1}})$ ), we upgrade the time modulus.

**Lemma 6.4** (Uniform strong time modulus). *There is  $C_T > 0$ , independent of  $u \in \mathcal{U}_{ad}^{BV}$ , with  $\|x^u(t+h, \cdot) - x^u(t, \cdot)\|_{L^1(\Omega)} \leq C_T h^{1/2}$  for  $0 \leq t \leq t+h \leq T$ .*

**Proposition 6.5** (Strong state compactness). *The set  $\mathcal{X}_T^{BV} := \{x^u : u \in \mathcal{U}_{ad}^{BV}\}$  is relatively compact in  $C([0, T]; L^1(\Omega))$ ; in particular every  $(u_n) \subset \mathcal{U}_{ad}^{BV}$  has a subsequence with  $x^{u_n} \rightarrow \bar{x}$  strongly in  $C([0, T]; L^1(\Omega))$ .*

*Remark 6.6* (Controls weak, states strong). The compactification produces  $u_n \xrightarrow{*} u$  in  $L^\infty$  together with  $x^{u_n} \rightarrow x^u$  strongly in  $C([0, T]; L^1)$ . No time-compactness or strong convergence of  $u_n$  is claimed; the strong state convergence is what permits passage to  $u_n x^{u_n}$ .

### 6.3 Sequential closedness

**Proposition 6.7** (Weak-\*/strong closedness). *If  $u_n \in \mathcal{U}_{ad}^{BV}$  and  $u_n \xrightarrow{*} u$  in  $L^\infty((0, T) \times \Omega)$ , then, after extraction,  $x^{u_n} \rightarrow x^u$  strongly in  $C([0, T]; L^1(\Omega))$ , where  $x^u$  is the state of the limit  $u \in \mathcal{U}_{ad}^{BV}$ .*

*Proof* By Proposition 6.5,  $x^{u_n} \rightarrow \bar{x}$  strongly, hence

$$E^{u_n}(t) = \int_{\Omega} \chi x^{u_n}(t, \cdot) \rightarrow \bar{E}(t) := \int_{\Omega} \chi \bar{x}(t, \cdot)$$

uniformly on  $[0, T]$ , so  $g(E^{u_n}, \cdot) \rightarrow g(\bar{E}, \cdot)$  and  $\mu(E^{u_n}, \cdot) \rightarrow \mu(\bar{E}, \cdot)$  uniformly. For the bilinear term, write, for bounded  $\psi$ ,

$$\int_0^T \int_{\Omega} u_n x^{u_n} \psi = \int_0^T \int_{\Omega} u_n \bar{x} \psi + \int_0^T \int_{\Omega} u_n (x^{u_n} - \bar{x}) \psi.$$

Since  $\bar{x}\psi \in L^1$ , weak-\* convergence handles the first term; the second is bounded by  $u_{\max} \|\psi\|_{\infty} \|x^{u_n} - \bar{x}\|_{L^1} \rightarrow 0$ . Passing to the limit in the weak formulation shows  $\bar{x}$  solves the state equation with control  $u$ , so  $\bar{x} = x^u$  by uniqueness; the limit being independent of the subsequence gives the claim.  $\square$

### 6.4 Existence of an optimal control

**Theorem 6.8** (Existence in  $\mathcal{U}_{ad}^{BV}$ ). *Under the hypotheses of Theorem 4.8 with  $c \in L^{\infty}_+(\Omega)$ , there is  $u_T^* \in \mathcal{U}_{ad}^{BV}$  with  $J_T(u_T^*) = V_T^{BV} = \sup_{u \in \mathcal{U}_{ad}^{BV}} J_T(u)$ .*

*Proof* Let  $(u_n) \subset \mathcal{U}_{ad}^{BV}$  be maximizing. By Lemma 6.1,  $u_n \xrightarrow{*} u_T^* \in \mathcal{U}_{ad}^{BV}$ ; by Proposition 6.7,  $x^{u_n} \rightarrow x^{u_T^*}$  strongly in  $C([0, T]; L^1)$ . Writing

$$\int_0^T \int_{\Omega} e^{-rt} c u_n x^{u_n} = \int_0^T \int_{\Omega} e^{-rt} c u_n x^{u_T^*} + \int_0^T \int_{\Omega} e^{-rt} c u_n (x^{u_n} - x^{u_T^*}),$$

the first term converges by weak-\* convergence (since  $e^{-rt} c x^{u_T^*} \in L^1$ ) and the second to zero by strong  $L^1$  convergence, so  $J_T(u_n) \rightarrow J_T(u_T^*) = V_T^{BV}$ .  $\square$

### 6.5 Scope of the compactification

Theorem 6.8 establishes existence for the restricted problem only; we do not prove  $V_T^{BV} = V_T$  nor that an unrestricted optimizer lies in  $\mathcal{U}_{ad}^{BV}$ . The relation is  $V_T^{BV} \leq V_T$ , with equality not established. We accordingly read all first-order results below as an optimality theory for  $\mathcal{U}_{ad}^{BV}$ . In particular, the ecological conclusions of Section 10 should be read as “among policies of bounded spatial complexity, an optimum exists and (conditionally) is minimum-size,” not as a statement about the unrestricted optimum.

*Remark 6.9* (Alternative relaxed formulations). Measure-valued harvesting controls provide an alternative route when optimal sequences develop concentrations or fine oscillations [36, 57, 58]; developing that relaxation and deciding equality with  $V_T^{BV}$  is beyond our scope.

## 6.6 Threshold policies

For minimum-size controls, compactness can be imposed on the threshold itself:

$$\mathcal{L}_{ad} := \{L \in BV(0, T) : l_0 \leq L(t) \leq l_m \text{ a.e.}, \text{TV}_{(0, T)}(L) \leq C_L\},$$

with  $\|u_{L_1} - u_{L_2}\|_{L^1((0, T) \times \Omega)} = u_{\max} \int_0^T |L_1 - L_2|$ .

**Proposition 6.10** (Existence in the threshold class). *There is  $L_T^* \in \mathcal{L}_{ad}$  with  $J_T(u_{L_T^*}) = \sup_{L \in \mathcal{L}_{ad}} J_T(u_L)$ .*

*Remark 6.11* (Stationary threshold). For a stationary threshold  $L \in [l_0, l_m]$  no temporal compactification is needed:  $[l_0, l_m]$  is compact and  $L \mapsto J_{\text{st}}(L)$  continuous, so a maximizer exists. Section 9 determines when it is consistent with the full nonlocal switching condition.

## 7 Adjoint and bang–bang variational inequality

We derive first-order conditions for  $\sup_{u \in \mathcal{U}_{ad}^{BV}} J_T(u)$ . Maximum principles and bang–bang laws are well established for related models [23, 29, 30, 32, 59, 60]; the distinctive feature is the nonlocal term created when the environment enters the rates. The correct general condition is a variational inequality over the tangent cone of  $\mathcal{U}_{ad}^{BV}$ ; a pointwise bang–bang rule follows only when the spatial-variation constraint is inactive.

We emphasize at the outset that this finite-horizon adjoint theory is conditional. The nonlocal functional (45) pairs a measure  $D_l x^*$  with the costate, and the single-crossing analysis treats  $S^*(t, \cdot)$  as continuous in size; both require  $\lambda^*(t, \cdot) \in C(\Omega)$ , which—as Remark 7.6 shows—can fail under the spatial- $BV$  control class. We therefore carry an explicit size-continuity hypothesis (R) throughout this section. The stationary theory of Section 9 is free of this issue: its adjoint is an ODE with bounded coefficients and is absolutely continuous, hence continuous in size, even for bang–bang  $u(l)$ .

Let  $u^* \in \mathcal{U}_{ad}^{BV}$  be optimal (Theorem 6.8), with  $x^* := x^{u^*}$  and  $E^*(t) := \int_{\Omega} \chi x^*(t, \cdot)$ . Following [5], who note that solution operators of size-structured consumer–resource models may fail to be differentiable in general, we impose the clean regularity that the rates depend smoothly on  $E$  as maps into the spatial spaces dictated by the characteristic argument:

$$c \in C^1(\Omega), \quad \chi \in C(\Omega), \quad E \mapsto g(E, \cdot) \in C^1(\mathbb{R}_+; W^{1, \infty}(\Omega)), \quad E \mapsto \mu(E, \cdot) \in C^1(\mathbb{R}_+; L^\infty(\Omega)), \quad (41)$$

and  $x^* \in L^\infty(0, T; BV(\Omega)) \cap L^\infty((0, T) \times \Omega)$ . The  $C^1(\mathbb{R}_+; W^{1, \infty}(\Omega))$  hypothesis on  $g$  supplies not only the zeroth-order expansion of  $g$  but the first-order expansion of  $\partial_l g$  in  $E$  needed by the characteristic attenuation, replacing a list of separate mixed-derivative bounds. We additionally assume the optimal-state costate regularity

$$\lambda^* \in C([0, T]; C(\Omega)), \quad (\text{R})$$

discussed and justified in Remark 7.6.

## 7.1 Linearized state equation

For a feasible bounded direction  $h$  of finite spatial variation, set  $u^\varepsilon = u^* + \varepsilon h$ ,  $x^\varepsilon = x^{u^\varepsilon}$ ,  $E^\varepsilon = \int_\Omega \chi x^\varepsilon$ , and let  $z = \lim_{\varepsilon \downarrow 0} (x^\varepsilon - x^*)/\varepsilon$ ,  $\delta E(t) = \int_\Omega \chi z(t, \cdot)$ . Formal differentiation gives

$$\partial_t z + \partial_l(g(E^*, l)z) + \partial_l(\partial_E g(E^*, l)x^* \delta E) = -(\mu(E^*, l) + u^*)z - \partial_E \mu(E^*, l)x^* \delta E - hx^*, \quad (42)$$

with  $z(0, \cdot) = 0$  and, since the inflow flux is control-independent,

$$g(E^*, l_0)z(t, l_0) + \partial_E g(E^*, l_0)x^*(t, l_0^+) \delta E(t) = 0. \quad (43)$$

**Proposition 7.1** (Directional differentiability). *For every bounded feasible direction  $h$  of finite spatial variation, the difference quotient  $(x^{u^* + \varepsilon h} - x^*)/\varepsilon$  converges in  $C([0, T]; L^1(\Omega))$  to the unique weak solution  $z$  of (42)–(43).*

## 7.2 Nonlocal adjoint and its $BV$ interpretation

We use a current-value costate  $\lambda$ , related to the present-value costate by  $\lambda_{pv} = e^{-rt}\lambda$ , which produces the  $-r\lambda$  term below. Dualizing the  $\delta E$  terms produces the formal scalar feedback

$$\Gamma(t) := \int_{l_0}^{l_m} [\partial_E g(E^*, \xi) \partial_\xi \lambda(t, \xi) - \partial_E \mu(E^*, \xi) \lambda(t, \xi)] x^*(t, \xi) d\xi, \quad (44)$$

giving the formal current-value adjoint

$$-\partial_t \lambda - g(E^*, l) \partial_l \lambda = c u^* - (r + \mu(E^*, l) + u^*) \lambda + \chi(l) \Gamma(t), \quad \lambda(T, \cdot) = 0, \lambda(t, l_m) = 0.$$

Since  $x^*(t, \cdot) \in BV(\Omega)$  and  $\lambda$  is only continuous, the derivative  $\partial_\xi \lambda$  in (44) is interpreted via a  $BV$  integration-by-parts. With  $G_t(l) := \partial_E g(E^*(t), l) \in C^1(\Omega)$ , the product  $G_t x^*(t, \cdot) \in BV(\Omega)$  with  $D_l(G_t x^*) = G_t D_l x^* + \partial_l G_t x^* dl$ .

**Definition 7.2** (Nonlocal adjoint functional). For  $\lambda(t, \cdot) \in C(\Omega)$ ,

$$\begin{aligned} \mathcal{G}_{x^*}[\lambda](t) := & -\partial_E g(E^*, l_0) \lambda(t, l_0) x^*(t, l_0^+) - \int_{[l_0, l_m]} \lambda(t, \xi) \partial_E g(E^*, \xi) D_l x^*(t, d\xi) \\ & - \int_{l_0}^{l_m} \lambda(t, \xi) [\partial_\xi \partial_E g(E^*, \xi) + \partial_E \mu(E^*, \xi)] x^*(t, \xi) d\xi. \end{aligned} \quad (45)$$

When  $x^*, \lambda$  are smooth,  $\mathcal{G}_{x^*}[\lambda]$  agrees with (44), the  $l_m$ -boundary term vanishing by  $\lambda(t, l_m) = 0$ .

**Lemma 7.3** (Boundedness). *There is  $C_\Gamma > 0$  with  $|\mathcal{G}_{x^*}[\lambda](t)| \leq C_\Gamma \|\lambda(t, \cdot)\|_{C(\Omega)}$  for a.e.  $t$ .*

The adjoint used below is

$$-\partial_t \lambda - g(E^*, l) \partial_l \lambda = c u^* - (r + \mu(E^*, l) + u^*) \lambda + \chi(l) \mathcal{G}_{x^*}[\lambda](t), \quad \lambda(T, \cdot) = 0, \quad \lambda(t, l_m) = 0. \quad (46)$$

**Assumption 7.4** (Continuous transient adjoint). The nonlocal adjoint equation (46) admits a unique solution  $\lambda^* \in C([0, T]; C(\Omega))$ , absolutely continuous along adjoint characteristics.

Assumption 7.4 is what (R) encodes; we state it as a hypothesis rather than a theorem because, as Remark 7.6 shows, it can fail under the spatial- $BV$  control class and we do not prove a coefficient/control condition that forces it. Under Assumption 7.4 the functional  $\mathcal{G}_{x^*}[\lambda^*]$  pairs the continuous  $\lambda^*$  with the finite measure  $D_l x^*$  and is well defined (Lemma 7.3), and the gradient representation and finite-horizon single-crossing results below are valid. We record what a genuine proof would require.

*Remark 7.5* (Toward a non-assumed continuous adjoint). A genuine well-posedness theorem would assume a property of the coefficients and of  $u^*$  ensuring that, for every prescribed scalar source  $\gamma \in C([0, T])$ , the local terminal-value transport solution  $\lambda[\gamma]$  lies in  $C([0, T]; C(\Omega))$  and that  $\gamma \mapsto \lambda[\gamma]$  is bounded  $C([0, T]) \rightarrow C([0, T]; C(\Omega))$ ; the contraction  $\gamma \mapsto \mathcal{G}_{x^*}[\lambda[\gamma]]$  (which has a short-time factor from the characteristic interval, by Lemma 7.3) would then deliver a continuous  $\lambda^*$ . The obstruction is exactly the carriage of a jump of  $c u^*$  along an adjoint characteristic to a fixed terminal size (Remark 7.6); a noncharacteristic-transversality condition on the switching curves of  $u^*$  removes it, but verifying such a condition is a regularity question for the optimal control that we do not settle here. Recent structured-population work likewise emphasizes that differentiability and regularity of these solution operators are delicate [5].

*Remark 7.6* (The costate need not be continuous in size; necessity of (R)). A uniform spatial- $BV$  bound on  $u^*$  does not by itself force  $\lambda^*(t, \cdot) \in C(\Omega)$ . Take constant speed  $g \equiv 1$  on  $\Omega$  and the one-switch control  $u^*(s, l) = \mathbf{1}_{\{l-s > \ell_c\}}$ , which has spatial variation 1 for every  $s$ , hence lies in  $\mathcal{U}_{ad}^{BV}$ . Along the adjoint characteristic  $l(s) = l + s - t$  one has  $u^*(s, l(s)) = \mathbf{1}_{\{l-t > \ell_c\}}$ , constant in  $s$  but discontinuous as a function of the terminal size  $l$  at  $l = t + \ell_c$ . The characteristic integral defining  $\lambda^*(t, l)$  therefore inherits a jump at  $l = t + \ell_c$ , so  $\lambda^*(t, \cdot) \notin C(\Omega)$  in general. Consequently (R) is a genuine restriction, not a consequence of the admissible class. It can be guaranteed by, e.g., restricting to controls continuous in size, or by a noncharacteristic-transversality condition on the switching curves of  $u^*$  (so that no jump of  $u^*$  is carried undamped along an adjoint characteristic to a fixed terminal size). When (R) fails, the finite-horizon costate must be handled in  $BV(\Omega)$  with a precise representative and a measure- $BV$  pairing in place of (45); we do not develop that here, and the affected results (Definition 7.2,

Assumption 7.4, continuity of  $S^*$ , and the finite-horizon single-crossing formulation) are stated under (R). None of the stationary results of Section 9 depends on it.

### 7.3 First variation

**Proposition 7.7** (Adjoint representation). *For every bounded feasible direction  $h$  of finite spatial variation,*

$$J'_T(u^*)h = \int_0^T e^{-rt} \int_{\Omega} x^*(t, l) S^*(t, l) h(t, l) dl dt, \quad S^*(t, l) := c(l) - \lambda^*(t, l).$$

### 7.4 Variational inequality and bang–bang

**Theorem 7.8** (First-order variational inequality). *For optimal  $u^* \in \mathcal{U}_{ad}^{BV}$ , with  $S^* = c - \lambda^*$ ,*

$$\int_0^T e^{-rt} \int_{\Omega} x^* S^*(v - u^*) dl dt \leq 0 \quad \text{for all } v \in \mathcal{U}_{ad}^{BV}. \quad (47)$$

If the variation budget is active, (47) cannot in general be reduced to a pointwise rule, and one writes the optimality condition abstractly as  $e^{-rt} x^* S^* \in N_{\mathcal{U}_{ad}^{BV}}(u^*)$ , the normal cone for the maximization convention.

**Theorem 7.9** (Bang–bang under an inactive constraint). *Suppose the variation constraint is inactive with a uniform margin,*

$$\operatorname{ess\,sup}_t \operatorname{TV}_{\Omega}(u^*(t, \cdot)) \leq C_u - \eta, \quad \eta > 0. \quad (48)$$

*Then for a.e.  $(t, l)$ ,  $u^*(t, l) \in \arg \max_{v \in [0, u_{\max}]} v x^*(t, l) S^*(t, l)$ , and where  $x^*(t, l) > 0$ ,*

$$u^*(t, l) = \begin{cases} 0, & S^*(t, l) < 0, \\ u_{\max}, & S^*(t, l) > 0. \end{cases} \quad (49)$$

*On the singular set  $\Sigma := \{S^* = 0\}$  the first-order condition does not determine  $u^*$ .*

**Remark 7.10** (Active constraint; singular arcs). If the budget is active, the normal cone contains a contribution from the  $BV$  constraint and (49) need not follow; the general condition remains (47). On  $\Sigma$ , determining the control requires higher-order or structural arguments, which we do not pursue.

### 7.5 Bang–bang does not imply a threshold

With  $\mathcal{H}_t := \{l : S^*(t, l) > 0\}$ , the bang–bang rule gives  $u^*(t, \cdot) = u_{\max} \mathbf{1}_{\mathcal{H}_t}$  off  $\Sigma$ , but  $\mathcal{H}_t$  may be several disjoint intervals. A minimum-size policy requires the stronger  $\mathcal{H}_t = (L^*(t), l_m]$ . Thus

inactive  $BV$  constraint + maximum principle  $\implies$  bang–bang harvesting,

and the threshold conclusion needs the single-crossing analysis of Section 8. Under the size-continuity hypothesis (R),  $S^* = c - \lambda^*$  is continuous in  $l$ , and the single-crossing geometry is then the only additional hypothesis; absent (R),  $S^*(t, \cdot)$  may jump (Remark 7.6), and the threshold formulation must be read for a precise representative of  $S^*$ .

## 8 Bang–bang versus threshold harvesting: the single-crossing condition

Under an inactive constraint, Theorem 7.9 gives the bang–bang law (49); we now ask when it is a minimum-size policy. The distinction is

$$\begin{aligned} \text{bang–bang} &\iff u^*(t, l) \in \{0, u_{\max}\} \text{ a.e.}, \\ \text{minimum-size} &\iff u^*(t, l) = u_{\max} \mathbf{1}_{\{l > L^*(t)\}} \text{ a.e.} \end{aligned}$$

### 8.1 Upward single crossing

**Definition 8.1** (Weak upward single crossing).  $S : \Omega \rightarrow \mathbb{R}$  has the weak upward single-crossing property if the ordered sign condition

$$l_1 < l_2 \implies \text{sgn } S(l_1) \leq \text{sgn } S(l_2), \quad \text{sgn } S \in \{-1, 0, 1\}, \quad (50)$$

holds; equivalently,  $\{l : S(l) < 0\}$  is a lower set and  $\{l : S(l) > 0\}$  is an upper set.

*Remark 8.2* (Why the one-sided implication is insufficient). The condition  $S(l_1) > 0 \implies S(l_2) \geq 0$  for  $l_1 < l_2$  does not characterize single crossing: a continuous  $S$  that is positive on  $(l_0, a)$  and then drops to and stays at 0 satisfies it, yet  $\{S > 0\} = (l_0, a)$  is not an upper set, and the sign pattern is positive-then-zero rather than negative|zero|positive. Requiring both that  $\{S < 0\}$  be a lower set and that  $\{S > 0\}$  be an upper set rules this out and is what Lemma 8.5 uses.

**Definition 8.3** (Strict upward single crossing). A continuous  $S$  has the strict property if either  $S < 0$  on  $\Omega$ , or  $S > 0$  on  $\Omega$ , or there is a unique  $L \in (l_0, l_m)$  with  $S < 0$  on  $(l_0, L)$ ,  $S(L) = 0$ ,  $S > 0$  on  $(L, l_m)$ .

**Assumption 8.4** (Single crossing of  $S^*$ ). For a.e.  $t$ ,  $l \mapsto S^*(t, l)$  is continuous and weakly upward single crossing.

Assumption 8.4 does not follow from the maximum principle; its validity depends on  $c$ , the state, the rates, and the full nonlocal adjoint. In the finite-horizon problem we retain it as an explicit hypothesis; the results that avoid it are the stationary ones of Section 9, unconditional only within the stationary canonical system.

## 8.2 Geometry and threshold structure

For fixed  $t$ , let  $L_-(t) := \sup\{l : S^*(t, l) < 0\}$ ,  $L_+(t) := \inf\{l : S^*(t, l) > 0\}$  (with  $\sup \emptyset = l_0$ ,  $\inf \emptyset = l_m$ ).

**Lemma 8.5** (Sign decomposition). *Let  $S^*(t, \cdot)$  be continuous and weakly upward single crossing in the sense of Definition 8.1. Then  $L_-(t) \leq L_+(t)$  and*

$$S^*(t, l) < 0 \quad (l < L_-), \quad S^*(t, l) = 0 \quad (L_- < l < L_+), \quad S^*(t, l) > 0 \quad (l > L_+), \quad (51)$$

with the endpoints determined as follows: if both sign sets  $\{S^* < 0\}$  and  $\{S^* > 0\}$  are nonempty, continuity gives  $S^*(L_-) = S^*(L_+) = 0$ ; if one sign set is empty, the corresponding endpoint coincides with a domain endpoint and  $S^*$  may take a strict sign there (e.g.  $L_- = L_+ = l_0$  and  $S^*(l_0) > 0$  when  $S^* > 0$  throughout, or  $L_- = L_+ = l_m$  and  $S^*(l_m) < 0$  when  $S^* < 0$  throughout). Conversely, for continuous  $S^*$  the existence of such  $L_- \leq L_+$  with (51) is equivalent to the ordered sign condition (50).

**Theorem 8.6** (Weak threshold structure). *Under Theorem 7.9 and Assumption 8.4, for a.e.  $t$  exactly one of the following holds, where  $x^*(t, \cdot) > 0$ :*

1.  $S^*(t, \cdot) \leq 0$  ( $\{S^* > 0\} = \emptyset$ ):  $u^*(t, \cdot) = 0$  off the zero set  $\{S^*(t, \cdot) = 0\}$ ;
2.  $S^*(t, \cdot) \geq 0$  ( $\{S^* < 0\} = \emptyset$ ):  $u^*(t, \cdot) = u_{\max}$  off the zero set;
3. both signs occur: with  $l_0 < L_-(t) \leq L_+(t) < l_m$ ,

$$u^*(t, l) = \begin{cases} 0, & l < L_-(t), \\ u_{\max}, & l > L_+(t), \end{cases}$$

and  $u^*$  undetermined on the singular interval  $(L_-(t), L_+(t)) \subseteq \{S^*(t, \cdot) = 0\}$ , on whose endpoints  $S^* = 0$ .

**Theorem 8.7** (Strict minimum-size policy). *Under Theorem 7.9, if  $S^*(t, \cdot)$  is strictly upward single crossing for a.e.  $t$ , then exactly one holds: (i)  $S^* < 0$  and  $u^* = 0$ ; (ii)  $S^* > 0$  and  $u^* = u_{\max}$ ; (iii) there is a unique  $L^*(t) \in (l_0, l_m)$  with  $S^*(t, L^*(t)) = 0$  and  $u^*(t, l) = u_{\max} \mathbf{1}_{\{l > L^*(t)\}}$  a.e.*

bang–bang optimality + strict upward single crossing  $\implies$  minimum-size harvesting.

## 8.3 Measurability and regularity

**Proposition 8.8** (Measurability). *If  $S^*$  is measurable in  $t$ , continuous in  $l$ , and weakly upward single crossing in  $l$  for a.e.  $t$ , then  $L_+$  and  $L_-$  are measurable.*

**Proposition 8.9** (Local regularity under transversal crossing). *If  $S^* \in C^1$  near  $(t_0, L^*(t_0))$  with  $S^* = 0$  and  $\partial_l S^* \neq 0$  there, then locally there is a unique  $C^1$  trajectory*

$L^*$  with  $S^*(t, L^*(t)) = 0$  and

$$\dot{L}^*(t) = -\frac{\partial_t S^*(t, L^*(t))}{\partial_l S^*(t, L^*(t))}. \quad (52)$$

Equation (52) is a local identity, not an independent evolution law, and fails at tangential or multiple crossings.

## 8.4 Monotonicity is sufficient but not necessary

**Proposition 8.10** (Single crossing is strictly weaker than monotonicity). *If  $S$  is strictly increasing it is strictly upward single crossing whenever it changes sign. The converse fails.*

## 8.5 A robust single-crossing certificate

**Proposition 8.11** (Quantitative certificate). *Let  $S \in C^1(\Omega)$  and suppose there are  $L \in (l_0, l_m)$ ,  $\delta, m, \kappa > 0$  with*

$$S(l) \leq -m, \quad l \in [l_0, L - \delta]; \quad S(l) \geq m, \quad l \in [L + \delta, l_m]; \quad S'(l) \geq \kappa, \quad l \in [L - \delta, L + \delta].$$

*Then  $S$  has exactly one zero in  $(L - \delta, L + \delta)$ , an upward crossing. Moreover any  $\tilde{S} \in C^1$  with  $\|\tilde{S} - S\|_{L^\infty} < m$  and  $\|\tilde{S}' - S'\|_{L^\infty(L - \delta, L + \delta)} < \kappa$  also has exactly one upward crossing.*

## 8.6 Switching geometries and the stationary route

For fixed  $t$ ,  $S^*$  may give: (i) no harvest ( $S^* < 0$ ); (ii) full harvest ( $S^* > 0$ ); (iii) a minimum-size regime; (iv) a singular band ( $S^* \equiv 0$  on an interval); or (v) a multiple-switch regime ( $\mathcal{H}_t$  disconnected). The last is the central caution: nonlocal feedback can alter the marginal value of one size class through its effect on all others, reshaping  $S^*$  enough to create extra crossings while the control stays bang–bang. Establishing single crossing uniformly in time would require control of the sign geometry of the nonlocal costate, so we retain it as a hypothesis in the time-dependent theory. In the stationary problem the adjoint is a linear ODE with scalar nonlocal feedback, which permits the exact decomposition  $S = S_{\text{red}} - \Gamma\psi$  developed next.

# 9 Stationary nonlocal switching correction

## 9.1 Which problem the stationary adjoint belongs to

The time-independent adjoint studied in this section carries a discount term  $r\lambda$  and therefore is not the adjoint of the finite-horizon problem  $J_T$  of Section 6, whose costate satisfies the terminal condition  $\lambda(T, \cdot) = 0$  and is generically nonstationary; nor is it the Lagrange multiplier of the static equilibrium-yield problem  $\max_u \int_\Omega c u x^u$ , in which  $r$  does not appear (multiplying a permanently stationary trajectory's value

$\int_0^\infty e^{-rt} \mathcal{Y}(u) dt = \mathcal{Y}(u)/r$  by  $1/r$  does not introduce an  $r\lambda$  term). The natural reading is the infinite-horizon discounted problem

$$J_\infty(u) = \int_0^\infty e^{-rt} \int_\Omega c(l) u(t, l) x(t, l) dl dt, \quad r > 0, \quad (53)$$

whose stationary canonical extremals are time-independent triples  $(x^*, E^*, u)$  together with a current-value costate  $\lambda$  solving the state equation, the current-value adjoint equation, and the pointwise maximum condition. Equation (57) below is exactly the stationary current-value canonical adjoint of (53) (equivalently, a resolvent/spectral-shift equation with parameter  $r \geq 0$ ). This section analyzes the switching geometry of such stationary canonical extremals; it does not by itself prove their global optimality, nor that a stationary extremal is optimal among nonstationary controls. Accordingly we speak throughout of stationary canonical bang–bang extremals, and a “minimum-size policy” conclusion is a statement about such an extremal, not a proved solution of a dynamic optimization.

**Definition 9.1** (Stationary canonical candidate). A quadruple  $(x^*, E^*, u, \lambda)$  is a stationary canonical candidate if  $E^* = \Phi(E^*)$  with profile  $x^* = x_{E^*}$ ,  $\lambda$  solves the stationary current-value adjoint (57), and the maximum (consistency) condition

$$u(l) \in \arg \max_{v \in [0, u_{\max}]} v x^*(l) S(l), \quad S := c - \lambda, \quad (54)$$

holds for a.e.  $l$ . The rank-one reduction below is valid for an arbitrary prescribed stationary  $u$ ; only the control-policy conclusions (that the harvested set is an upper interval) additionally invoke (54).

In the stationary problem the nonlocal feedback is scalar, allowing an exact rank-one reduction of the adjoint. We develop the reduction, small-feedback and certificate results, and the unification identity  $B|_{r=0} = \Phi'(E^*)$ .

## 9.2 Operating point

Fix a stationary policy  $u = u(l) \in [0, u_{\max}]$  and a stationary environment  $E^*$  with  $E^* = \Phi(E^*)$  and profile  $x^* = x_{E^*}$  as in (17). Unlike the transient problem, the stationary profile and stationary costate are absolutely continuous in size: since  $(\bar{g}x^*)' = -(\bar{\mu} + u)x^* \in L^\infty(\Omega)$  and  $\bar{g} \geq g_{\min}$  one has  $x^* \in W^{1,\infty}(\Omega)$ , and the stationary terminal-value ODEs below give  $\lambda, \psi \in W^{1,\infty}(\Omega)$ . We therefore define the stationary feedback functional directly by its strong form, with no measure pairing and no appeal to the transient continuity hypothesis (R). Write

$$\bar{g} := g(E^*, \cdot), \quad \bar{\mu} := \mu(E^*, \cdot), \quad g_E := \partial_E g(E^*, \cdot), \quad \mu_E := \partial_E \mu(E^*, \cdot),$$

and the discounted-mortality coefficient (this is the symbol freed by the renaming in Section 3), defined for  $r \geq 0$  by

$$a_r(l) := r + \bar{\mu}(l) + u(l) \geq 0, \quad \text{with } a_r \geq r > 0 \text{ for } r > 0.$$

The original discounted control problem has  $r > 0$ ; the value  $r = 0$  is used below only as the zero-shift limit in the closure-gain identity, and the terminal-value ODEs remain well posed there because  $\bar{g} \geq g_{\min} > 0$ . We write  $a_r$  throughout to make the dependence of  $\psi_r$ ,  $B(r)$ , and the spectral shift explicit, abbreviating  $a := a_r$  when  $r$  is fixed. For  $\zeta \in W^{1,\infty}(\Omega)$  define the stationary feedback functional by

$$\mathcal{G}^*[\zeta] := \int_{l_0}^{l_m} (g_E(\xi)\zeta'(\xi) - \mu_E(\xi)\zeta(\xi))x^*(\xi) d\xi, \quad (55)$$

which is well defined and bounded on  $W^{1,\infty}(\Omega)$  because  $x^* \in W^{1,\infty}(\Omega) \subset L^\infty(\Omega)$  and  $g_E, \mu_E \in L^\infty(\Omega)$ . When  $x^*$  is only  $BV$  (the transient situation), an integration by parts gives the equivalent  $BV$  representation

$$\mathcal{G}^*[\zeta] = -g_E(l_0)\zeta(l_0)x^*(l_0^+) - \int_{[l_0, l_m]} \zeta(\xi)g_E(\xi) D_l x^*(d\xi) - \int_{l_0}^{l_m} \zeta(\xi)(g'_E(\xi) + \mu_E(\xi))x^*(\xi) d\xi, \quad (56)$$

agreeing with (55) for  $x^* \in W^{1,\infty}$ ; we use the strong form (55) as the foundation of this section and regard (56) as an equivalent representation. The full stationary current-value adjoint is

$$\bar{g}(l)\lambda'(l) = a(l)\lambda(l) - c(l)u(l) - \chi(l)\Gamma, \quad \lambda(l_m) = 0, \quad \Gamma = \mathcal{G}^*[\lambda]. \quad (57)$$

### 9.3 Reduced adjoint and response function

Define  $\lambda_{\text{red}}$  and  $\psi$  by

$$\bar{g}\lambda'_{\text{red}} = a\lambda_{\text{red}} - cu, \quad \lambda_{\text{red}}(l_m) = 0, \quad (58)$$

$$\bar{g}\psi' = a\psi - \chi, \quad \psi(l_m) = 0, \quad (59)$$

with explicit solutions

$$\lambda_{\text{red}}(l) = \int_l^{l_m} \frac{c(s)u(s)}{\bar{g}(s)} \exp\left(-\int_l^s \frac{a}{\bar{g}}\right) ds, \quad \psi(l) = \int_l^{l_m} \frac{\chi(s)}{\bar{g}(s)} \exp\left(-\int_l^s \frac{a}{\bar{g}}\right) ds, \quad (60)$$

both nonnegative for  $c, u, \chi \geq 0$ . Set  $S_{\text{red}}(l) := c(l) - \lambda_{\text{red}}(l)$ .

*Remark 9.2* (Interpretation of  $\psi$ ).  $\psi$  is the costate response to one unit of the scalar nonlocal source; it propagates the environmental correction backward from larger sizes. The full nonlocal effect has fixed shape  $\psi$ , with magnitude and sign set by the scalar  $\Gamma$ .

## 9.4 Exact rank-one correction

Define

$$A := \mathcal{G}^*[\lambda_{\text{red}}], \quad B := \mathcal{G}^*[\psi], \quad (61)$$

with smooth forms

$$A = \int_{l_0}^{l_m} (g_E \lambda'_{\text{red}} - \mu_E \lambda_{\text{red}}) x^* d\xi, \quad B = \int_{l_0}^{l_m} (g_E \psi' - \mu_E \psi) x^* d\xi.$$

**Theorem 9.3** (Rank-one correction). *If  $1 - B \neq 0$ , the full stationary adjoint (57) has the unique representation*

$$\lambda = \lambda_{\text{red}} + \Gamma \psi, \quad \Gamma = \frac{A}{1 - B},$$

so that

$$S = S_{\text{red}} - \frac{A}{1 - B} \psi, \quad S' = S'_{\text{red}} - \frac{A}{1 - B} \psi'. \quad (62)$$

*Remark 9.4* (Sherman–Morrison and nonresonance). The closure  $\Gamma = A + \Gamma B$  of Theorem 9.3 is the scalar Sherman–Morrison identity [61] made precise as follows. Let  $L_0$  denote the reduced terminal-value operator, so that  $\lambda_{\text{red}} = L_0^{-1}(cu)$  and  $\psi = L_0^{-1}\chi$ , and let  $\mathcal{G}^*$  act as a bounded linear functional. The full adjoint solves the rank-one-perturbed equation

$$(I - \psi \otimes \mathcal{G}^*)\lambda = \lambda_{\text{red}}, \quad (\psi \otimes \mathcal{G}^*)\lambda := \psi \mathcal{G}^*[\lambda],$$

whose inverse is  $(I - \psi \otimes \mathcal{G}^*)^{-1} = I + \frac{\psi \otimes \mathcal{G}^*}{1 - \mathcal{G}^*[\psi]}$ , with denominator  $1 - \mathcal{G}^*[\psi] = 1 - B$ . Applying it to  $\lambda_{\text{red}}$  reproduces  $\lambda = \lambda_{\text{red}} + \frac{A}{1 - B} \psi$  since  $\mathcal{G}^*[\lambda_{\text{red}}] = A$ . If  $B = 1$  and  $A \neq 0$  the closure is inconsistent; if  $B = 1$  and  $A = 0$  the adjoint is algebraically nonunique. Hence uniqueness forces  $B \neq 1$ . The correction is rank one for every  $B \neq 1$ ; rank one does not mean small, since  $|\Gamma| = |A|/|1 - B|$  can be large near resonance.

## 9.5 Quantitative feedback bounds

From (62),

$$\|S - S_{\text{red}}\|_{L^\infty} \leq \frac{|A|}{|1 - B|} \|\psi\|_{L^\infty}, \quad \|S' - S'_{\text{red}}\|_{L^\infty} \leq \frac{|A|}{|1 - B|} \|\psi'\|_{L^\infty},$$

with  $\psi' = (a\psi - \chi)/\bar{g}$ , hence  $\|\psi'\|_\infty \leq (\|a\|_\infty \|\psi\|_\infty + \|\chi\|_\infty)/g_{\min}$  and  $0 \leq \psi \leq \|\chi\|_\infty (l_m - l_0)/g_{\min}$ .

**Lemma 9.5** (Feedback vanishes with the sensitivities). *If a uniformly bounded family of operating points satisfies  $\|g_E\|_{C^1} + \|\mu_E\|_{L^\infty} \leq \varepsilon$ , then there is  $C > 0$  with  $|A| + |B| \leq C\varepsilon$ , and for small  $\varepsilon$ ,  $|\Gamma| \leq C\varepsilon/(1 - C\varepsilon) = O(\varepsilon)$ .*

## 9.6 Small-feedback preservation of single crossing

**Theorem 9.6** (Monotone case). *If  $S'_{\text{red}} \geq \eta > 0$  on  $(l_0, l_m)$ ,  $|B| \leq \beta < 1$ , and  $\frac{|A|}{1-\beta} \|\psi'\|_{L^\infty} < \eta$ , then  $S' > 0$ , so  $S$  has at most one zero; if also  $S(l_0) < 0 < S(l_m)$ , then  $S$  has exactly one upward crossing. If, in addition, the operating point is a stationary canonical candidate (Definition 9.1, i.e. the consistency condition (54) holds), the corresponding stationary canonical bang–bang extremal is a minimum-size policy.*

**Theorem 9.7** (Nonmonotone case). *Suppose there are  $L_{\text{red}} \in (l_0, l_m)$ ,  $\delta, m, \kappa > 0$  with  $S_{\text{red}} \leq -m$  on  $[l_0, L_{\text{red}} - \delta]$ ,  $S_{\text{red}} \geq m$  on  $[L_{\text{red}} + \delta, l_m]$ , and  $S'_{\text{red}} \geq \kappa$  on  $[L_{\text{red}} - \delta, L_{\text{red}} + \delta]$ . If  $B \neq 1$ ,  $\frac{|A|}{|1-B|} \|\psi\|_{L^\infty} < m$ , and  $\frac{|A|}{|1-B|} \|\psi'\|_{L^\infty([L_{\text{red}}-\delta, L_{\text{red}}+\delta])} < \kappa$ , then  $S$  has exactly one upward crossing in  $(L_{\text{red}} - \delta, L_{\text{red}} + \delta)$ ; if the operating point is a stationary canonical candidate (consistency condition (54)), the corresponding stationary canonical bang–bang extremal is a minimum-size policy.*

**Corollary 9.8** (Weak feedback). *Under Lemma 9.5, if  $S_{\text{red}}$  has a robust upward crossing (the margins of Theorem 9.7), there is  $\varepsilon_0 > 0$  such that every operating point with  $\|g_E\|_{C^1} + \|\mu_E\|_\infty < \varepsilon_0$  has a full switching function with exactly one upward crossing.*

## 9.7 Threshold displacement

**Proposition 9.9** (First-order displacement). *If  $S_{\text{red}}(L_{\text{red}}) = 0$ ,  $S'_{\text{red}}(L_{\text{red}}) \neq 0$ , and the correction is small enough for a unique nearby zero  $L^*$  to exist, then  $L^* - L_{\text{red}} = \frac{\Gamma\psi(L_{\text{red}})}{S'_{\text{red}}(L_{\text{red}})} + O(\Gamma^2)$ .*

The first-order displacement of the switching threshold is illustrated in Figure 3. The spy inset highlights the horizontal shift  $L^* - L_{\text{red}}$  caused by the vertical rank-one perturbation  $-\Gamma\psi(l)$ , consistently with the approximation in Proposition 8.7.

## 9.8 Unification: the closure gain is the zero-discount feedback gain

We now prove that the feedback gain  $B$  and the closure derivative  $\Phi'(E^*)$  of Section 3 are the same scalar at zero discount, with  $r$  acting as a spectral shift. Write  $\alpha = -g_E/\bar{g} \geq 0$  and  $b$  as in (20)–(21), both evaluated at  $E^*$ , and let  $\tau(\xi, s) := \int_\xi^s d\eta/\bar{g}(\eta)$  be the growth time from  $\xi$  to  $s$ . For  $r \geq 0$  let  $\psi_r$  solve (59) with  $a = r + \bar{\mu} + u$ , and  $B(r) := \mathcal{G}^*[\psi_r]$  (smooth form (55)). Define the discounted tail load

$$W_r(\xi) := \int_\xi^{l_m} \chi(s) x^*(s) e^{-r\tau(\xi, s)} ds, \quad W_0 = W_{E^*}. \quad (63)$$

**Lemma 9.10** (Forward/adjoint survival duality). *For every  $r \geq 0$  and  $\xi \in \Omega$ ,  $\bar{g}(\xi) \psi_r(\xi) x^*(\xi) = W_r(\xi)$ . In particular, at  $r = 0$ ,  $\bar{g} \psi x^* = W_{E^*}$ .*

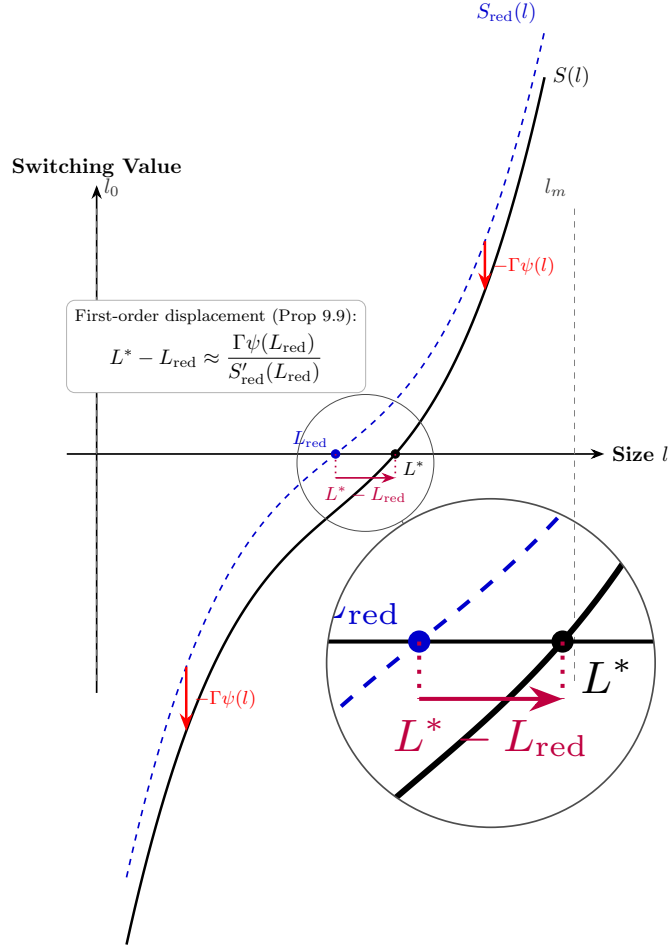


**Fig. 3** Displacement of switching thresholds. The spy inset magnifies the first-order shift  $L^* - L_{\text{red}}$  between  $S(l)$  and  $S_{\text{red}}(l)$  induced by the rank-one perturbation  $-\Gamma\psi(l)$ .

**Theorem 9.11** (Closure-gain identity). *Let  $A^* := A(E^*)$  and  $C^* := C(E^*)$ . For every  $r \geq 0$ ,*

$$B(r) = \underbrace{\int_{l_0}^{l_m} \alpha \chi x^*}_{A^*} - \int_{l_0}^{l_m} b(\xi) W_r(\xi) \, d\xi - r \int_{l_0}^{l_m} \frac{\alpha(\xi)}{\bar{g}(\xi)} W_r(\xi) \, d\xi. \quad (64)$$

*In particular,*

$$B(0) = A^* - C^* = \Phi'(E^*).$$

*If, in addition,  $\chi x^*$  is continuous and  $\bar{g}$  is continuous and bounded below on  $\Omega$  (so that  $\xi \mapsto \chi(\xi)x^*(\xi)\bar{g}(\xi)$  is bounded and the inner integrand below is dominated uniformly),*

then  $\lim_{r \rightarrow \infty} B(r) = 0$ :

$$B(0) = \Phi'(E^*), \quad \lim_{r \rightarrow \infty} B(r) = 0.$$

**Corollary 9.12** (Automatic and unconditional nonresonance).

1. If the local condition  $\Phi'(E^*) < 0$  holds at the operating point, then  $1 - B(0) = 1 - \Phi'(E^*) > 1$ , and by continuity there is  $r_0 > 0$  with  $1 - B(r) > 0$  for  $r \in [0, r_0]$ . This holds in particular whenever the global integrated-monotonicity condition of Theorem 3.7 is satisfied, but only the local sign of  $\Phi'$  at  $E^*$  is needed here.
2. (Unconditional in  $r$ .) Since  $\alpha, b, W_r \geq 0$ , the two subtracted terms in (64) are nonnegative, so  $B(r) \leq A^*$  for all  $r \geq 0$ . Hence

$$A^* = \int_{l_0}^{l_m} \left( -\frac{gE}{g} \right) \chi x^* dl < 1 \quad \implies \quad 1 - B(r) > 0 \quad \text{for all } r \geq 0.$$

*Remark 9.13* (Characteristic-equation reading and its limits). Because  $B$  carries no payoff ( $A$  alone carries the source  $cu$ ),  $B(r)$  is the scalar loop gain of the stationary closure at spectral shift  $r$ , and  $1 - B(r) = 0$  has the form of a closure/characteristic equation; at  $r = 0$  it reduces to  $1 - \Phi'(E^*)$ . The condition  $\Phi'(E^*) < 0$  thus controls only the  $r = 0$  slice, i.e. the zero-discount closure. An all- $r$  guarantee is equivalent to the absence of a nonnegative real root of  $1 - B(r)$  and does not follow from  $\Phi'(E^*) < 0$  in general. Formula (64) does not imply monotonicity of  $B(r)$  under the present assumptions, because discounting acts differently on spatially separated contributions: indeed  $B(r) - B(0) = \int b(W_0 - W_r) - r \int \frac{\alpha}{g} W_r$  has a sign that need not be definite, the first term being nonnegative and the second nonpositive. The robust, operating-point-checkable guarantee is therefore Corollary 9.12(b); the neighborhood guarantee of part (a) is the consequence of steady-state uniqueness alone.

## 9.9 Reconstruction and certificate

For a prescribed stationary  $u$ : (1) solve  $E^* = \Phi(E^*)$  and form  $x^*$ ; (2) solve (58) for  $\lambda_{\text{red}}$ ; (3) solve (59) for  $\psi$ ; (4) evaluate  $A, B$  from (61); (5) check  $d := 1 - B$ ; (6) if  $d \neq 0$ , set  $\Gamma = A/d$  and  $S = S_{\text{red}} - \Gamma\psi$ ; (7) read the sign geometry of  $S$ . The residual  $R_{\text{rank}} := \|\lambda - \lambda_{\text{red}} - \Gamma\psi\|_{L^\infty}$  is zero in exact arithmetic and serves as an implementation check.

**Definition 9.14** (Grid diagnostic). A grid diagnostic computes  $\lambda_{\text{red}}, \psi, A, B, \Gamma, S$  on a fine mesh and records the observed sign changes of  $S$ . It is evidence for, not a proof of, single crossing.

For a rigorous certificate, partition  $l_0 = \ell_0 < \dots < \ell_N = l_m$ ,  $I_j = [\ell_{j-1}, \ell_j]$ , and suppose validated computations produce interval enclosures  $[S](I_j) \supseteq \{S(l) : l \in I_j\}$ ,  $[S'](I_j)$ , and  $[A], [B], [\Gamma]$  with  $0 \notin 1 - [B]$ .

**Theorem 9.15** (Validated single-crossing certificate). *If there is a unique  $k$  with  $\sup[S](I_j) < 0$  for  $j < k$ ,  $\inf[S](I_j) > 0$  for  $j > k$ ,  $\inf[S'](I_k) > 0$ , and  $S(\ell_{k-1}) < 0 < S(\ell_k)$ , then  $S$  has exactly one zero in  $I_k$ , an upward crossing; if the operating point is a stationary canonical candidate (54), the corresponding stationary canonical bang–bang extremal is a minimum-size policy.*

**Corollary 9.16** (Endpoint policies). *Suppose the operating point is a stationary canonical candidate (54). If  $\sup[S](I_j) < 0$  for all  $j$ , then  $S < 0$  and the extremal is no harvesting; if  $\inf[S](I_j) > 0$  for all  $j$ , then  $S > 0$  and the extremal is full harvesting.*

**Proposition 9.17** (Multiple-switch certificate). *If for ordered  $q_1 < q_2 < q_3$  validated enclosures give  $S(q_1) < 0 < S(q_2)$  and  $S(q_2) > 0 > S(q_3)$  (or the reversed pattern), then  $S$  has at least two zeros and fails single crossing.*

## 9.10 Near-resonance and conditioning

The denominator  $d = 1 - B$  must be monitored: for perturbations,  $\delta\Gamma = \frac{\delta A}{1 - B} + \frac{A \delta B}{(1 - B)^2} + \dots$ , so reconstruction is ill-conditioned as  $B \rightarrow 1$ . A certificate should report  $A, B, 1 - B, \Gamma, |A|/|1 - B|$  with validated error bounds. Near resonance, a small change in the sensitivities produces a large change in  $S$ : this identifies a regime of high marginal feedback gain in which the minimum-size policy is structurally fragile.

## 9.11 Summary

The apparently nonlocal stationary adjoint reduces to two local terminal-value ODEs and one scalar closure  $\Gamma = A + \Gamma B$ , giving, under  $1 - B \neq 0$ ,

$$\Gamma = \frac{A}{1 - B}, \quad S = S_{\text{red}} - \frac{A}{1 - B}\psi, \quad B|_{r=0} = \Phi'(E^*).$$

This furnishes an exact reconstruction of the switching function, small-feedback single-crossing criteria, a threshold-displacement formula, diagnostics for multiple-switch and no-threshold regimes, a validated certificate, and the identification of the closure gain with the discounted feedback gain. The reduction holds for any prescribed stationary control; the minimum-size conclusion applies to any stationary canonical bang–bang extremal of the infinite-horizon discounted problem (Definition 9.1). The conclusion is not that nonlocality always preserves a minimum-size extremal, nor that a stationary extremal is globally optimal, but that the exact scalar correction—anchored to the classical closure derivative—identifies precisely when single crossing holds and when it does not.

## 10 Ecological and numerical consequences

We now instantiate the theory in a calibrated, density-dependent von Bertalanffy [62, 63] model and use it to extract ecological consequences. The aim of this section

is not to confirm the preceding theorems—the rank-one reduction and the identity  $B|_{r=0} = \Phi'(E^*)$  are exact—but to use them as instruments that expose a concrete, and previously implicit, ecological trade-off and to map the circumstances under which a conventional minimum-size harvest rule remains valid.

## 10.1 Calibrated model

Lengths are in centimetres and time in years. Growth is von Bertalanffy with multiplicative crowding suppression, mortality is additive in the environmental load, and the environment is a biomass-weighted competition index:

$$g(E, l) = \frac{k(L_\infty - l)}{1 + \rho_g E}, \quad \mu(E, l) = \mu_0 + \rho_\mu E, \quad \chi(l) = \left(\frac{l}{l_m}\right)^3, \quad E = \int_{l_0}^{l_m} \chi(l)x(l) dl.$$

Because  $L_\infty > l_m$ , growth is bounded below by  $g_{\min}(M) = k(L_\infty - l_m)/(1 + \rho_g M) > 0$  on each bounded environmental interval  $[0, M]$ , which is the local form of (7); the stationary analysis uses it on the closure interval  $[0, M_{\text{st}}]$ , with  $M_{\text{st}} = \Phi(0)$  (the maximum of the decreasing closure map, computed per parameter set), and the finite-horizon analysis uses it on  $[0, M_T]$ . Its infimum over all  $E \geq 0$  is zero, so no global floor is claimed; one could impose a global floor by the variant  $g = k(L_\infty - l)[\varepsilon_g + (1 - \varepsilon_g)/(1 + \rho_g E)]$  with  $\varepsilon_g > 0$ , which we do not need here. The compensatory signs (9) hold with  $\partial_E g = -k(L_\infty - l)\rho_g/(1 + \rho_g E)^2 \leq 0$  and  $\partial_E \mu = \rho_\mu \geq 0$ . Fecundity is given by  $m(l) = (l/l_m)^3/(1 + e^{-(l-l_{50})/\delta_m})$ . The realised value per harvested individual is taken in two forms: a monotone form  $c(l) = (l/l_m)^3$  (value rising with body weight) and a dome-shaped form  $c(l) = \exp(-((l - l_{\text{val}})/w_{\text{val}})^2)$  representing a harvest value peaked at an intermediate size  $l_{\text{val}}$  (for instance a size-graded market premium). We emphasise that this dome enters the payoff  $c$  only; it is not a gear-selectivity constraint on the feasible fishing mortality. Baseline parameters and ranges are listed in Table 1; all quantities below are computed on a length grid with the trapezoidal closure and the exact terminal-value adjoints of Section 9.

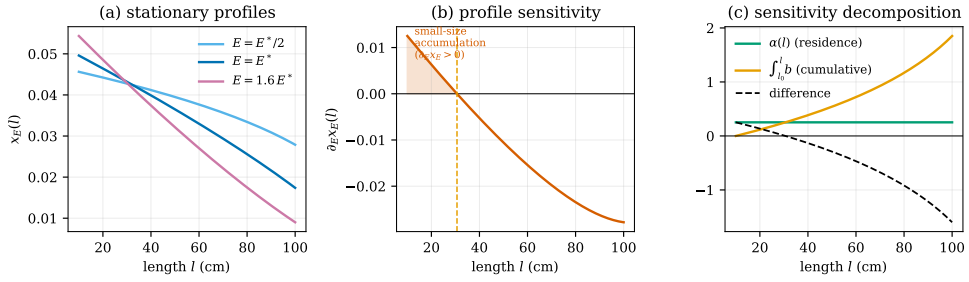
## 10.2 The biological mechanism

Figure 4 displays the mechanism at the unfished operating point ( $E^* \approx 0.63$ ). As the environmental load rises, the stationary profile (panel a) does not fall uniformly: near the recruitment size, the density strictly increases. This occurs because the boundary fixes the entering flux while crowding-suppressed growth raises the residence density  $p/g(E, l_0)$  of recruits. The sensitivity  $\partial_E x_E$  (panel b) is therefore positive over an inflow band—about 21 cm wide at the unfished point (spanning from the recruitment size  $l_0 = 10$  cm to a crossover at  $l \approx 31$  cm) and about 24 cm wide under the computed canonical harvest—and negative thereafter. Panel (c) resolves this into the two competing integrals of Section 3: a positive residence-time term  $\alpha = -\partial_E g/g$  concentrated near  $l_0$ , and a negative cumulative term  $\int_{l_0}^l b$  that accrues with size as mortality and delayed progression remove individuals from the larger classes. Their crossover is the boundary of the small-size accumulation region.

**Table 1** Model parameters: definitions, units, baseline values, plausible ranges, and basis. The environment  $E$  is a dimensionless biomass-weighted competition index; feedback coefficients  $\rho_g, \rho_\mu$  are calibrated so that the crowding factors  $1 + \rho_g E$  and the mortality increment  $\rho_\mu E$  are of order one at the operating point.

Symbol	Definition	Unit	Baseline	Range
$l_0, l_m$	recruitment / exit size	cm	10, 100	fixed
$k$	von Bertalanffy rate	yr <sup>-1</sup>	0.20	0.14–0.26
$L_\infty$	asymptotic length	cm	130	121–139 <sup>†</sup>
$\mu_0$	baseline mortality	yr <sup>-1</sup>	0.20	0.14–0.26
$\rho_g$	growth-suppression feedback	–	0.30	0–3
$\rho_\mu$	mortality-increase feedback	–	0.15	0–0.8
$u_{\max}$	maximum fishing mortality	yr <sup>-1</sup>	0.40	0.28–0.52
$r$	discount rate	yr <sup>-1</sup>	0.05	0.02–0.08
$p$	recruitment flux	yr <sup>-1</sup>	1 (norm.)	fixed
$l_{50}, \delta_m$	maturity ogive	cm	45, 5	—
$l_{\text{val}}, w_{\text{val}}$	dome harvest-value centre / width	cm	52, 16	30–90

<sup>†</sup> In the uncertainty study  $L_\infty$  is sampled as  $l_m$  plus a  $\pm 30\%$  perturbation of the growth gap  $L_\infty - l_m$ , which keeps  $L_\infty > l_m$  and hence  $g > 0$  throughout the size range.



**Fig. 4** Biological mechanism. (a) Stationary profiles  $x_E$  at increasing environmental load; the inflow density rises with  $E$ . (b) Profile sensitivity  $\partial_E x_E$ , positive over a small-size accumulation band (shaded) and negative beyond it. (c) Decomposition of  $\partial_E \log x_E$  into the local residence-time gain  $\alpha$  and the cumulative survival/progression loss  $\int_{l_0}^l b$ .

Whether this local accumulation overturns global behaviour is decided by the integrated balance  $\Phi'(E) = A(E) - C(E)$  of Theorem 3.7. Figure 5 shows the closure map  $\Phi$  crossing the identity once and the decomposition  $A - C$  remaining negative across the relevant range: at baseline  $A \approx 0.16$  while  $C \approx 0.72$ , so  $\Phi'(E^*) \approx -0.56$  and the steady state is unique. The accumulation near the inflow is genuine but the cumulative loss dominates the integral.

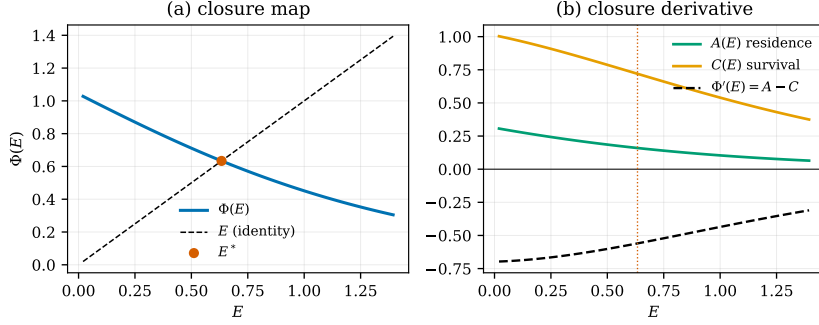


**Fig. 5** Stationary closure. (a)  $\Phi(E)$  meets the identity once at  $E^*$ . (b) The residence amplification  $A$ , the cumulative reduction  $C$ , and  $\Phi' = A - C < 0$ : uniqueness holds because the cumulative loss exceeds the inflow gain.

### 10.3 Where the mechanism matters

Figure 6 maps the mechanism over the feedback plane  $(\rho_g, \rho_\mu)$ . To probe uniqueness as a global property—rather than only the local slope at the fixed point—panel (a) shows the sufficient-condition diagnostic  $\max_{E \in [0, M_{\text{st}}]} \Phi'(E)$  of Theorem 3.7, evaluated on the stationary closure interval  $[0, M_{\text{st}}]$  with  $M_{\text{st}} = \Phi(0)$  recomputed for each parameter pair: where it is negative,  $\Phi' < 0$  throughout  $[0, M_{\text{st}}]$  and the steady state is unique. It is negative over all but  $\approx 4.4\%$  of the sampled plane, the exception being the extreme growth-limited corner (large  $\rho_g$ , negligible  $\rho_\mu$ ) where the residence amplification  $A$ , although saturating ( $\alpha = \rho_g / (1 + \rho_g E)$ ), is no longer dominated by the cumulative loss across the whole interval. At the no-feedback corner  $\rho_g = \rho_\mu = 0$  the rates are  $E$ -independent and  $\Phi' \equiv 0$ , so the condition is non-strict there. At the computed fixed point the local slope  $\Phi'(E^*)$  is nonpositive throughout the plane and strictly negative away from the no-feedback corner. The width of the small-size accumulation region (panel b), by contrast, grows steadily with  $\rho_g$  and can exceed a third of the size range: the accumulation phenomenon is widespread even though it does not destabilise the equilibrium.

### 10.4 Switching correction and harvest policy

For monotone value, the reduced switching function is increasing and the rank-one correction  $-\Gamma\psi$  is a modest positive shift ( $\Gamma \approx -0.08$ ,  $1 - B \approx 1.25$ , far from resonance): a single upward crossing survives and the canonical extremal is a minimum-size policy (Figure 7a; the maximum-condition residual is zero to machine precision). This is not special to the baseline: at every resolved point of the feedback plane, policy iteration returned a verified minimum-size stationary canonical candidate. The picture changes when the harvest value is dome-shaped and peaks at small sizes. Protecting small individuals then no longer lets them grow into a more valuable class, and the canonical switching function acquires additional crossings (Figure 7b shows a self-consistent two-crossing extremal, residual zero): the computed stationary canonical candidate is a harvested window, not a threshold.

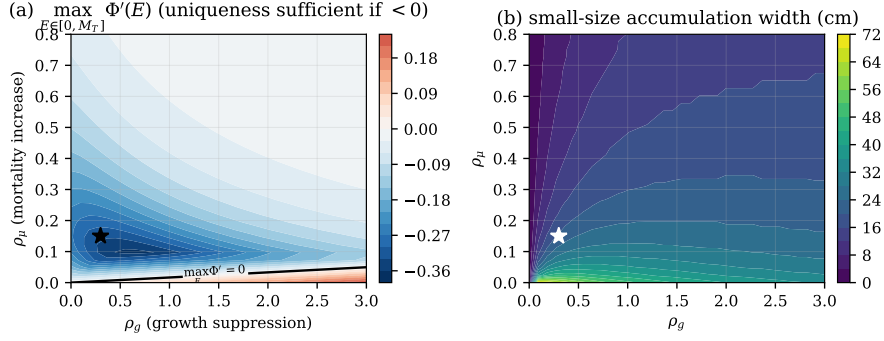


**Fig. 6** Mechanism map over  $(\rho_g, \rho_\mu)$  (star: baseline). (a) The sufficient-uniqueness diagnostic  $\max_{E \in [0, M_{\text{st}}]} \Phi'(E)$  on the stationary closure interval ( $M_{\text{st}} = \Phi(0)$ ) per parameter pair: negative (hence  $\Phi' < 0$  throughout  $[0, M_{\text{st}}]$  and the equilibrium unique) over all but the extreme growth-limited corner. (b) Width (cm) of the small-size accumulation region, which broadens with growth suppression.

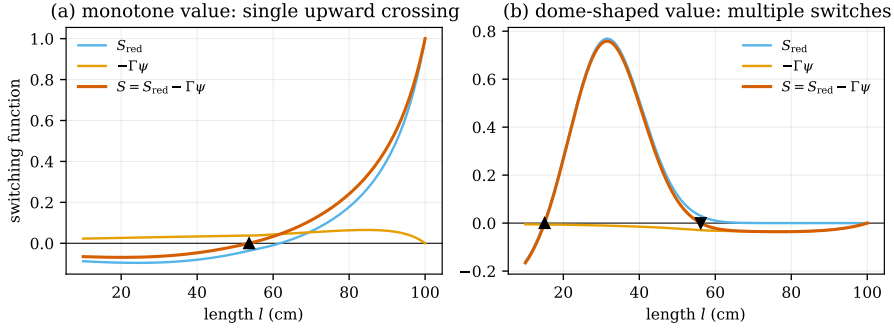


**Fig. 7** Rank-one switching correction  $S = S_{\text{red}} - \Gamma\psi$ . (a) Monotone value: a single upward crossing (minimum-size policy). (b) Dome-shaped value peaked at small sizes: the correction yields multiple crossings, i.e. a harvested size window rather than a threshold (markers: upward  $\blacktriangle$  / downward  $\blacktriangledown$  crossings). Both panels are self-consistent canonical extremals (maximum-condition residual zero).

Figure 8 classifies the canonical extremal across the dome-value plane  $(\rho_g, l_{\text{val}})$  using self-consistent policy iteration. Minimum-size policies occupy  $\approx 90.7\%$  of the plane; a band of multiple-switch (window) policies ( $\approx 7.7\%$ ) appears where the value peak sits at small sizes, and a thin set of cases ( $\approx 1.7\%$ ) does not reach a verified fixed point and is labelled unconverged rather than counted as a regime. Where the window regime occurs, the computed stationary canonical candidate is not a minimum-size policy, demonstrating that the canonical conditions do not generally enforce threshold structure; the transition is the loss of single crossing flagged by the fine-grid diagnostic of Section 9 (a grid-level sign-pattern test, not the interval-validated certificate of Theorem 9.15, which we do not implement numerically here).

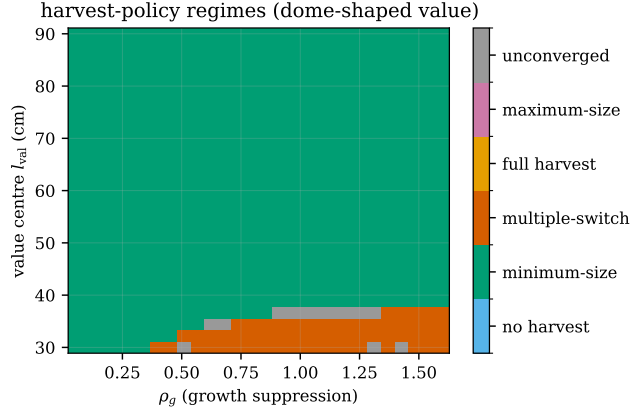


**Fig. 8** Harvest-policy regimes under dome-shaped value over  $(\rho_g, l_{\text{val}})$ , from self-consistent policy iteration. Minimum-size policies dominate; window (multiple-switch) policies appear when the value peak is at small sizes; unconverged cases are shown separately. Failed computations are excluded (none occurred), not coded as a regime.

## 10.5 Ecological trade-offs

Figure 9 traces the consequences of strengthening feedback (scaling  $\rho_g, \rho_\mu$  jointly). Equilibrium yield and biomass fall as feedback intensifies; the computed canonical threshold  $L^*$  shifts downward, so stronger compensation calls for protecting less of the size range; and the replacement diagnostics decline. Two replacement quantities must be distinguished. The equilibrium-adjusted spawning-potential ratio  $\text{SPR}_{\text{eq}}$  stays near 0.5 across the range (baseline 0.53); because its numerator and denominator are evaluated at different equilibrium environments, this is not the conventional fixed-vital-rate SPR and is not by itself a sustainability criterion. The invasion replacement quantity, by contrast, is  $\mathcal{R}_0(u) = \mathcal{R}(0; u) \approx 0.415 < 1$  at baseline; moreover the replacement functional satisfies  $\sup_{E \in [0, M_{\text{st}}]} \mathcal{R}(E; u) = 0.415 < 1$  (the maximum is at  $E = 0$ ), so the harvested stock fails to replace itself at every environment in the closure interval. The forced model nevertheless maintains a positive stationary population through the prescribed recruitment flux  $p$ : a moderate equilibrium-adjusted SPR coexists with failure of low-density (indeed all-density) replacement. This is the forced-persistence caveat of Section 5, made quantitative. Representative regimes are summarised in Table 2.

## 10.6 Numerical validation and robustness

The exact results provide stringent internal checks. The unification identity  $B|_{r=0} = \Phi'(E^*)$  holds to machine precision (residual  $5 \times 10^{-16}$ ). The algebraic reconstruction  $\lambda = \lambda_{\text{red}} + \Gamma\psi$  is exact by construction, so  $\|\lambda - \lambda_{\text{red}} - \Gamma\psi\|_\infty$  is zero in floating point and is not an independent test; we instead report the  $\Gamma$ -consistency (closure) residual  $|\mathcal{G}^*[\lambda] - \Gamma|$ , which probes the discrete closure and is  $\sim 10^{-17}$  (Table 3). Recomputing the canonical solution at each resolution, the operating point and rank-one scalars are stable to approximately  $10^{-3}$  by  $N = 800$ . The successive changes are small but

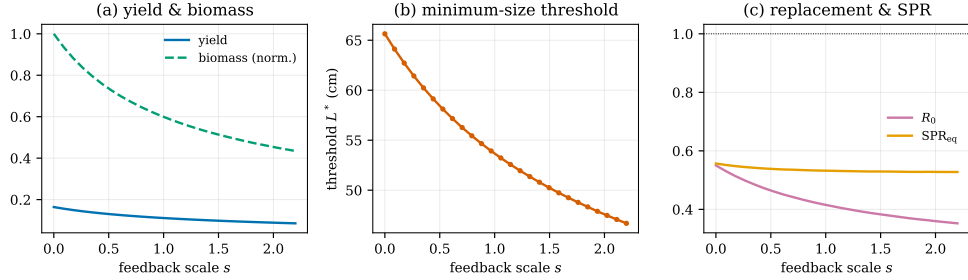


**Fig. 9** Ecological trade-offs versus feedback strength  $s$  (joint scaling of  $\rho_g, \rho_\mu$ ). (a) Yield and (normalised) biomass decline. (b) The computed canonical threshold  $L^*$  falls. (c) The equilibrium-adjusted SPR stays near 0.5 while the invasion replacement quantity  $\mathcal{R}_0$  remains below one: a moderate equilibrium-adjusted SPR coexists with failure of low-density replacement.

**Table 2** Representative regimes (all computed as self-consistent canonical extremals by policy iteration).  $E^*$ , the closure derivative  $\Phi'(E^*)$ , its parts  $A, C$ , the rank-one scalars  $A, B, 1 - B, \Gamma$ , the policy type, the ecological outputs (yield, biomass,  $\mathcal{R}_0$ ,  $\text{SPR}_{\text{eq}}$ ), and the maximum-condition residual “res” (mismatch fraction; zero indicates an exact canonical fixed point on the grid). The two dome rows use the dome payoff  $c$  at baseline feedback with the value peak at an intermediate size (“baseline peak”,  $l_{\text{val}} = 52$ ) and at a small size (“small-size peak”,  $l_{\text{val}} = 30$ ,  $\rho_g = 1$ ); the former is a minimum-size candidate, the latter a self-consistent harvested window (the case of Figure 7b).

Regime	$E^*$	$\Phi'$	A	C	A	B	$1 - B$	$\Gamma$
Baseline	0.361	-0.266	0.098	0.364	-0.0946	-0.2470	1.247	-0.0759
Weak feedback	0.484	-0.112	0.046	0.158	-0.0390	-0.1047	1.105	-0.0353
Growth-limited	0.380	-0.243	0.265	0.508	-0.1065	-0.2423	1.242	-0.0857
Mortality-limited	0.264	-0.431	0.026	0.457	-0.1465	-0.3913	1.391	-0.1053
Strong symmetric	0.240	-0.496	0.161	0.657	-0.1795	-0.4573	1.457	-0.1232
Dome value, baseline peak	0.259	-0.205	0.072	0.277	-0.0862	-0.1899	1.190	-0.0725
Dome value, small-size peak	0.280	-0.516	0.219	0.735	0.0343	-0.4556	1.456	0.0235

Regime	policy	yield	biom.	$\mathcal{R}_0$	SPR	res
Baseline	min-size	0.1111	0.361	0.415	0.532	0.0e+00
Weak feedback	min-size	0.1393	0.484	0.488	0.542	0.0e+00
Growth-limited	min-size	0.1088	0.380	0.426	0.480	0.0e+00
Mortality-limited	min-size	0.0871	0.264	0.360	0.564	0.0e+00
Strong symmetric	min-size	0.0792	0.240	0.338	0.528	0.0e+00
Dome value, baseline peak	min-size	0.2692	0.259	0.272	0.369	0.0e+00
Dome value, small-size peak	multi-switch	0.3075	0.280	0.412	0.490	0.0e+00

non-monotone at finer resolutions, associated with the grid-dependent placement of the switching point, so the present experiment does not provide a clean empirical convergence-order estimate; a dedicated rate study would align the switch with each grid and integrate separately on either side.

Robustness to parameter uncertainty is assessed by Monte-Carlo sampling ( $\pm 30\%$  uniform on  $k, \mu_0, \rho_g, \rho_\mu, u_{\text{max}}$ , and on the growth gap  $L_\infty - l_m$  so that  $L_\infty > l_m$  and  $g > 0$  throughout; Figure 10). Each draw is solved with the window-admitting policy

**Table 3** Mesh convergence and residuals (canonical solution recomputed at each resolution).

Columns: grid size  $N$ ; operating point  $E^*$ ; closure derivative  $\Phi'(E^*)$ ; gain  $B$ ; correction  $\Gamma$ ; successive change  $|E_N^* - E_{N/2}^*|$ ; observed order; the  $\Gamma$ -consistency (closure) residual  $|\mathcal{G}^*[\lambda] - \Gamma|$ ; and the identity residual  $|B(0) - \Phi'(E^*)|$ . The successive change is small ( $\lesssim 10^{-4}$ ) but non-monotone, reflecting grid-dependent placement of the switch; we therefore do not claim a clean empirical convergence order.

$N$	$E^*$	$\Phi'(E^*)$	$B$	$\Gamma$	$ \Delta E^* $	order	$\gamma$ -res	id-res
200	0.36127	-0.26620	-0.24698	-0.07589	2.29e-04	–	0.0e+00	0.0e+00
400	0.36130	-0.26623	-0.24700	-0.07589	2.00e-04	1.20	1.4e-17	0.0e+00
800	0.36131	-0.26624	-0.24701	-0.07589	1.88e-04	1.11	2.8e-17	1.1e-16
1600	0.36132	-0.26624	-0.24702	-0.07589	1.82e-04	-4.96	1.4e-17	3.3e-16
3200	0.36150	-0.26636	-0.24713	-0.07591	–	–	1.4e-17	5.0e-16

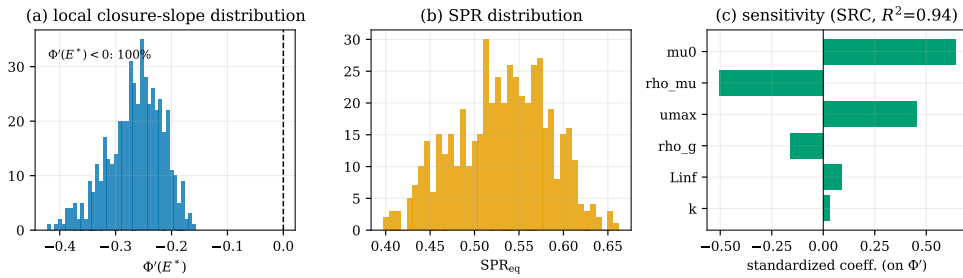


**Fig. 10** Robustness ( $\pm 30\%$  admissible parameter sampling,  $L_\infty > l_m$  enforced). (a) Distribution of the local closure slope  $\Phi'(E^*)$ : negative in all admissible draws. (b) Distribution of  $\text{SPR}_{\text{eq}}$ . (c) Standardized-regression sensitivity of  $\Phi'(E^*)$  to the sampled parameters (linear fit  $R^2 = 0.94$ ).

iteration and its maximum-condition residual is verified. The local closure slope  $\Phi'(E^*)$  is negative in all admissible draws, so the equilibrium is locally unique throughout the sample; the equilibrium SPR has median 0.53; and a standardized-regression sensitivity analysis (linear fit  $R^2 = 0.94$ ) ranks  $\mu_0$ ,  $\rho_\mu$ , and  $u_{\text{max}}$  as the dominant controls on the closure derivative, with  $L_\infty$  now minor—the earlier prominence of  $L_\infty$  was an artifact of draws that violated  $L_\infty > l_m$ . Because the solver admits harvest windows, the finding that every admissible draw returns a minimum-size canonical extremal is a genuine result, not an artifact of a threshold-only search.

## 10.7 Ecological conclusion

The analysis identifies a previously hidden ecological trade-off. Crowding-induced growth suppression increases the residence density of small individuals near the recruitment size, whereas elevated mortality and delayed progression remove individuals from the larger size classes. The integrated balance of these two effects—not the sign of either feedback alone—determines whether the stationary equilibrium is unique, how far intrinsic replacement falls below the equilibrium spawning-potential ratio, and

whether a conventional minimum-size harvest rule remains the canonical policy. In the calibrated model the balance is robustly tipped toward the cumulative loss, so the equilibrium is unique and the minimum-size rule survives for value that rises with size; yet the same feedback drives the intrinsic basic reproduction number under the computed canonical harvest below one, so the exploited stock persists only through recruitment subsidy, and when the harvest value peaks at small sizes the computed canonical candidate is a harvested window rather than a threshold. These distinctions are invisible to a pointwise or fixed-vital-rate analysis and are made quantitative here by the closure derivative  $\Phi'(E^*) = A - C$  and its exact identity with the discounted feedback gain.

We provide detailed proofs for all the mathematical conclusions in the main text.

## A Proofs in Section 3

*Proof of Proposition 3.1* The transformation  $y_E = g(E, \cdot)x_E$  reduces the equation to a scalar linear ODE with unique solution  $p\sigma_E$ . Dividing by  $g(E, l) > 0$  gives (17); since  $0 < \sigma_E \leq 1$  and  $g \geq g_{\min}(M_{\text{st}})$  on  $[0, M_{\text{st}}] \times \Omega$ , the bound follows.  $\square$

*Proof* Proof of Proposition 3.2 Continuity on  $[0, M_{\text{st}}]$  follows from continuity of  $g, \mu$  in  $E$ , the positive lower bound  $g_{\min}(M_{\text{st}})$  of (7), and dominated convergence. By (H-st) the continuous  $F(E) := \Phi(E) - E$  satisfies  $F(0) = \Phi(0) \geq 0$  and  $F(M_{\text{st}}) = \Phi(M_{\text{st}}) - M_{\text{st}} \leq 0$ , so the intermediate value theorem gives a fixed point. Positivity follows from  $x_E > 0$ .  $\square$

*Proof of Proposition 3.5* At  $l = l_0$  the cumulative integral in (22) vanishes, giving  $\partial_E \log x_E(l_0) = \alpha(E, l_0) \geq 0$ ; multiplying by  $x_E(l_0) > 0$  gives (23). Strictness and the local statement follow from  $\partial_E g(E, l_0) < 0$  and continuity of the bracket.  $\square$

*Proof of Theorem 3.7* Strict decrease follows from (24); existence from Proposition 3.2. Two fixed points  $E_1 < E_2$  would give  $E_1 = \Phi(E_1) > \Phi(E_2) = E_2$ , a contradiction. Uniqueness of the profile is Proposition 3.1.  $\square$

## B Proofs in Section 4

*Proof of Lemma 4.2 Amplitude.* The attenuation exponent  $\mathcal{A}_E(a, t; l) = \exp(-\int_a^t (\partial_l g + \mu + u))$  need not be  $\leq 1$ , since  $\partial_l g$  may be negative; using  $\mu + u \geq 0$  and  $(\partial_l g) \geq -(\partial_l g)^-$ ,

$$0 \leq \mathcal{A}_E(a, t; l) \leq \exp\left(\int_a^t \|(\partial_l g(E(s), \cdot))^- \|_{L^\infty} ds\right) \leq e^{T\|\partial_l g\|_{L^\infty}}, \quad (65)$$

so  $x$  is bounded by  $\max(\|\phi\|_\infty, \sup_s p(s)/g_{\min}) e^{T\|\partial_l g\|_\infty} =: C_T^0$ ; all amplitude estimates hold with this larger constant.

*Existence of the one-sided trace.* Boundedness alone does not give a trace; we argue from the representation (28). As  $l \uparrow l_m$ , the backward characteristic footpoint  $\eta_E(0; t, l)$  and the entrance time  $\tau_E(t, l)$  have one-sided limits (each is monotone in  $l$ );  $\phi \in BV$  and  $p \in BV$  have one-sided limits at those footpoints; for a.e.  $s$ ,  $u(s, \cdot) \in BV(\Omega)$  has a one-sided trace along the characteristic; and the attenuation integral converges by dominated convergence using (65). Hence  $x(t, l_m^-) = \lim_{l \uparrow l_m} x(t, l)$  exists for a.e.  $t$  and is bounded; multiplying by  $g \leq g_{\max}$  gives  $\beta \in L^\infty(0, T)$ .

*Green identity.* Multiply (12) by  $\psi \in W^{1,\infty}(\Omega)$ , integrate over  $(t, t+h) \times \Omega$ , and integrate the flux term by parts in  $l$ ; the boundary contributions are the prescribed inflow flux  $g(E, l_0)x(\cdot, l_0) = p$  at  $l_0$  and the outflow flux  $\beta$  at  $l_m$  (which exists by the previous step). The manipulation does not require  $\psi(l_m) = 0$ , giving (27).  $\square$

*Proof of Lemma 4.3* Existence, uniqueness, and nonnegativity follow from (28). The  $L^1$  bound is the population estimate; the  $L^\infty$  bound uses the bounded data,  $g \geq g_{\min}$ , and the attenuation bound (65) (which is  $\leq e^{T\|\partial_l g\|_\infty}$ , not necessarily  $\leq 1$ ). The outflow trace bound is Lemma 4.2. None of these uses a variation bound on  $E$ .  $\square$

*Proof of Lemma 4.5* Apply the Green identity (27) with  $\psi = \chi \in W^{1,\infty}(\Omega)$  on  $(t, t+h)$ , divide by  $h$ , and let  $h \downarrow 0$ : the left side tends to  $(\mathcal{F}E)'(t)$  at Lebesgue points, the interior terms to  $\int_\Omega (gx_E \chi' - (\mu + u)x_E \chi)$ , the inflow term to  $\chi(l_0)p(t)$ , and the outflow term to  $-\chi(l_m)g(E, l_m)x_E(t, l_m)$ , giving (30). The bound (31) follows from  $|p| \leq \|p\|_\infty$ , the trace bound  $g(E, l_m)x_E(\cdot, l_m) \leq C_T^0$ , and the  $L^1$  and pointwise bounds on  $x_E$ , all from (29); every constant is independent of  $E$ . Integrating gives the Lipschitz bound.  $\square$

*Proof of Lemma 4.6* Fix  $t$ . For  $s \leq t$  the map  $l \mapsto \eta_E(s; t, l)$  is monotone (characteristics do not cross), as are the footpoint and entrance-time maps; composition with a monotone map does not increase total variation, so  $\text{TV}_l(f(s, \eta_E(s; t, \cdot))) \leq \text{TV}_\Omega(f(s, \cdot))$  for any  $f(s, \cdot) \in BV(\Omega)$ , with  $f = \partial_l g + \mu + u$  giving  $\text{TV}_l \leq \|\partial_l g\|_{BV} + \|\mu\|_{BV} + C_u$ .

The attenuation exponent on the boundary-fed branch is  $H(l) = \int_{\tau_E(t, l)}^t f(s, \eta_E(s; t, l)) ds$ , whose lower limit moves with  $l$ . We prove the key estimate

$$\text{TV}_l H \leq \int_0^t \text{TV}_l(f(s, \eta_E(s; t, \cdot))) ds + \|f\|_{L^\infty} \text{TV}_l(\tau_E(t, \cdot)). \quad (66)$$

For a partition  $l_0 \leq a_0 < \dots < a_k \leq l_m$ , write each increment as

$$H(a_j) - H(a_{j-1}) = \underbrace{\int_{\tau_E(t, a_{j-1})}^t [f(s, \eta_E(s; t, a_j)) - f(s, \eta_E(s; t, a_{j-1}))] ds}_{\text{(I): common time interval}} - \underbrace{\int_{\tau_E(t, a_{j-1})}^{\tau_E(t, a_j)} f(s, \eta_E(s; t, a_j)) ds}_{\text{(II): differing lower limits}}.$$

Summing |(I)| over  $j$  and applying Fubini gives at most  $\int_0^t \text{TV}_l(f(s, \eta_E(s; t, \cdot))) ds$ ; summing |(II)| gives at most  $\|f\|_{L^\infty} \sum_j |\tau_E(t, a_j) - \tau_E(t, a_{j-1})| \leq \|f\|_{L^\infty} \text{TV}_l(\tau_E(t, \cdot))$ . Taking the supremum over partitions yields (66). The first term is bounded by  $T(\|\partial_l g\|_{BV} + \|\mu\|_{BV} + C_u)$  as above. For the second,  $\tau_E(t, \cdot)$  is monotone in  $l$  with values in  $[0, t]$ , so  $\text{TV}_l(\tau_E(t, \cdot)) \leq t \leq T$  directly from monotonicity (the maximum possible travel time), with no Lipschitz claim required. Hence  $\text{TV}_l H \leq C(T, C_u)$ , and  $\text{TV}(\mathcal{A}_E) \leq \|\mathcal{A}_E\|_\infty \text{TV}_l H$  since  $h \mapsto e^{-h}$  is Lipschitz on bounded sets and  $\mathcal{A}_E$  is bounded by (65).

For the boundary density, the  $L_E$ -Lipschitz bound on  $E$  makes  $t \mapsto 1/g(E(t), l_0)$  Lipschitz, hence of bounded variation, with  $\text{TV}_{(0, T)}(1/g(E(\cdot), l_0)) \leq g_{\min}^{-2} \|\partial_E g\|_\infty L_E T$ ; combined with  $p \in BV(0, T)$  and composition with the monotone map  $\tau_E(t, \cdot)$  (composition with a monotone map does not increase total variation), the boundary factor  $p(\tau_E)/g(E(\tau_E), l_0)$  has uniformly bounded spatial variation. The  $BV$  product rule, the  $BV$  datum  $\phi$ , and the single interface between initial-fed and boundary-fed characteristics (one jump of uniformly bounded size) then yield (32).  $\square$

*Proof of Lemma 4.7* Lipschitz dependence of  $g$  on  $E$  gives, for the flows and entrance-time maps,  $\sup_{s \leq t \leq \tau} \sup_l |\eta_{E_1} - \eta_{E_2}| \leq C_T \tau \|E_1 - E_2\|_C$ . Applying the translation estimate  $\|f(\cdot + h) - f\|_{L^1} \leq |h| \text{TV}(f)$  to the factors of (28) and using the uniform spatial- $BV$  bound of Lemma 4.6 (available because  $E_1, E_2 \in \mathcal{B}_{M_T}^{L_E}$ ) together with Lemma 4.3 yields (33).  $\square$

*Proof of Theorem 4.8* The contraction above on the closed set  $\mathcal{B}_{M_T}^{L_E}$  gives a unique fixed point  $E^u \in \mathcal{B}_{M_T}^{L_E}$  on a short interval; the population bound (15) prevents escape from  $\mathcal{B}_{M_T}$  and the uniform Lipschitz bound (31) prevents escape from  $\mathcal{B}_{M_T}^{L_E}$ , so the construction iterates over  $[0, T]$  with constants independent of the starting time. The amplitude bounds are Lemma 4.3; the spatial- $BV$  bound is Lemma 4.6, which applies precisely because  $E^u$  is  $L_E$ -Lipschitz.  $\square$

*Proof of Proposition 4.9* Work on a short interval  $[0, \tau]$  and iterate. Subtract the characteristic representations (28) of  $x_1, x_2$  along their respective flows  $\eta_1, \eta_2$  and reaction factors  $\mathcal{A}_1, \mathcal{A}_2$ . The control enters through the attenuation exponent evaluated along the characteristic; the essential point is that  $u_1, u_2$  are evaluated along different characteristics, so we split

$$u_1(s, \eta_1(s)) - u_2(s, \eta_2(s)) = \underbrace{[u_1(s, \eta_1(s)) - u_1(s, \eta_2(s))]}_{(a)} + \underbrace{[u_1(s, \eta_2(s)) - u_2(s, \eta_2(s))]}_{(b)}.$$

Term (a) is a spatial translation of the fixed  $BV$  function  $u_1(s, \cdot)$  by  $|\eta_1(s) - \eta_2(s)|$ ; the translation estimate  $\|w(\cdot + \delta) - w\|_{L^1} \leq |\delta| \text{TV}(w)$  and the uniform spatial- $BV$  bound  $\text{TV}_\Omega(u_1(s, \cdot)) \leq C_u$  bound its  $L^1$ -in- $l$  contribution by  $C_u \sup_s |\eta_1(s) - \eta_2(s)|$ . Since the flows depend on  $E_i$  through  $g$ ,  $\sup_{s \leq \tau} \sup_l |\eta_1 - \eta_2| \leq C_T \tau \|E_1 - E_2\|_C$ , and  $|E_1 - E_2| \leq \|\chi\|_\infty \|x_1 - x_2\|_{L^1}$ . Term (b) is evaluated along the common characteristic  $\eta_2$ ; a change of variables back to  $l$  bounds its contribution by  $C_T \|u_1 - u_2\|_{L^1((0, \tau) \times \Omega)}$ . Here the relevant change-of-variables Jacobian is  $\partial \eta_2(s; l) / \partial l$ , the derivative of the flow with respect to its initial size; by the variational equation  $\frac{d}{ds}(\partial_l \eta_2) = \partial_l g(E_2, \eta_2) \partial_l \eta_2$  it satisfies  $\exp(-\int_0^s \|\partial_l g\|_\infty) \leq \partial_l \eta_2 \leq \exp(\int_0^s \|\partial_l g\|_\infty)$ , so it is bounded above and below by the local bound on  $\partial_l g$  from (10) (not merely by the range of  $g$ ). The same split applied to the boundary factor  $p_i(\tau_{E_i})/g(E_i, l_0)$  gives, by (a)-type translation in the entrance time plus (b)-type direct difference, a bound  $C_T (\|p_1 - p_2\|_{L^1(0, \tau)} + \sup_s |\tau_{E_1} - \tau_{E_2}|)$  with  $\sup_s |\tau_{E_1} - \tau_{E_2}| \leq C_T \tau \|E_1 - E_2\|_C$ ; the initial-datum factor contributes  $\|\phi_1 - \phi_2\|_{L^1}$  directly. Collecting terms,

$$\|x_1 - x_2\|_{C([0, \tau]; L^1)} \leq C_T (\|\phi_1 - \phi_2\|_{L^1} + \|p_1 - p_2\|_{L^1} + \|u_1 - u_2\|_{L^1}) + C_T \tau \|x_1 - x_2\|_{C([0, \tau]; L^1)};$$

choosing  $\tau$  with  $C_T \tau \leq \frac{1}{2}$  absorbs the last term, and iterating over  $\lceil T/\tau \rceil$  intervals (with constants uniform under the common  $L^\infty$  and spatial- $BV$  bounds) gives (34).  $\square$

## C Proofs of Section 5

*Proof of Proposition 5.1* A stationary renewal profile is proportional to the unit-flux profile,  $x = b \hat{x}_E$ ; the renewal boundary condition (35) is homogeneous of degree one in  $x$  and reduces to  $\mathbf{A}(E; u) = 1$ , independent of  $b$ . The closure  $E = \int \chi x = b \int \chi \hat{x}_E$  then fixes the amplitude  $b$  as in (36), which is positive and finite when  $E^\dagger > 0$  and  $\int \chi \hat{x}_{E^\dagger} > 0$ . At  $E = 0$  a positive state would force  $\int \chi x > 0$ , contradicting  $E = 0$  when  $\chi > 0$  on a positive-measure set. Monotonicity in  $u$  follows since increasing  $u$  lowers the survival factor; strict monotonicity in  $E$  and the endpoint signs give a unique root by the intermediate value theorem.  $\square$

## D Proofs in Section 6

*Proof of Lemma 6.1* Convexity follows from convexity of the box constraint and subadditivity of total variation. By Banach–Alaoglu a bounded sequence has a weak-\* limit  $u$  with  $0 \leq u \leq u_{\max}$ ; passing to the limit in (37) keeps the variation bound, so  $u \in \mathcal{U}_{ad}^{BV}$ .  $\square$

*Proof of Lemma 6.3* Let  $\psi \in W^{1,\infty}(\Omega)$  with  $\|\psi\|_{W^{1,\infty}} \leq 1$ . The Green identity (27) of Lemma 4.2—valid for every  $\psi \in W^{1,\infty}(\Omega)$ , not only those vanishing at  $l_m$ —gives

$$\begin{aligned} \left| \int_{\Omega} (x^u(t+h, \cdot) - x^u(t, \cdot)) \psi \right| &\leq \int_t^{t+h} \int_{\Omega} g(E^u, l) x^u |\partial_l \psi| \, dl \, ds \\ &\quad + \int_t^{t+h} \int_{\Omega} (\mu(E^u, l) + u) x^u |\psi| \, dl \, ds \\ &\quad + \int_t^{t+h} p(s) |\psi(l_0)| \, ds + \int_t^{t+h} g(E^u(s), l_m) x^u(s, l_m^-) |\psi(l_m)| \, ds. \end{aligned}$$

The first three terms are bounded by  $C_T h$  using the uniform  $L^1$  state bound and boundedness of  $g, \mu, u, p$ . For the outflow term, Lemma 4.2 gives the trace bound  $g(E^u(s), l_m) x^u(s, l_m^-) \leq g_{\max} C_T$  in  $L^\infty(0, T)$ , so it too is bounded by  $C_T h$ . Taking the supremum over  $\psi$  gives (39).  $\square$

*Proof of Lemma 6.4* Apply (40) to  $v = x^u(t+h, \cdot) - x^u(t, \cdot)$ ; the weak norm is bounded by Lemma 6.3 and the  $L^1 + \text{TV}$  factor by (38).  $\square$

*Proof of Proposition 6.5* For each  $t$ , (38) and the compact embedding  $BV(\Omega) \hookrightarrow L^1(\Omega)$  give pointwise relative compactness; Lemma 6.4 gives equicontinuity of  $t \mapsto x^u(t, \cdot)$  into  $L^1(\Omega)$ . The vector-valued Arzelà–Ascoli theorem yields relative compactness in  $C([0, T]; L^1(\Omega))$ .  $\square$

*Proof of Proposition 6.7* By Proposition 6.5,  $x^{u_n} \rightarrow \bar{x}$  strongly, hence

$$E^{u_n}(t) = \int_{\Omega} \chi x^{u_n}(t, \cdot) \rightarrow \bar{E}(t) := \int_{\Omega} \chi \bar{x}(t, \cdot)$$

uniformly on  $[0, T]$ , so  $g(E^{u_n}, \cdot) \rightarrow g(\bar{E}, \cdot)$  and  $\mu(E^{u_n}, \cdot) \rightarrow \mu(\bar{E}, \cdot)$  uniformly. For the bilinear term, write, for bounded  $\psi$ ,

$$\int_0^T \int_{\Omega} u_n x^{u_n} \psi = \int_0^T \int_{\Omega} u_n \bar{x} \psi + \int_0^T \int_{\Omega} u_n (x^{u_n} - \bar{x}) \psi.$$

Since  $\bar{x} \psi \in L^1$ , weak-\* convergence handles the first term; the second is bounded by  $u_{\max} \|\psi\|_{\infty} \|x^{u_n} - \bar{x}\|_{L^1} \rightarrow 0$ . Passing to the limit in the weak formulation shows  $\bar{x}$  solves the state equation with control  $u$ , so  $\bar{x} = x^u$  by uniqueness; the limit being independent of the subsequence gives the claim.  $\square$

*Proof of Theorem 6.8* Let  $(u_n) \subset \mathcal{U}_{ad}^{BV}$  be maximizing. By Lemma 6.1,  $u_n \xrightarrow{*} u_T^* \in \mathcal{U}_{ad}^{BV}$ ; by Proposition 6.7,  $x^{u_n} \rightarrow x^{u_T^*}$  strongly in  $C([0, T]; L^1)$ . Writing

$$\int_0^T \int_{\Omega} e^{-rt} c u_n x^{u_n} = \int_0^T \int_{\Omega} e^{-rt} c u_n x^{u_T^*} + \int_0^T \int_{\Omega} e^{-rt} c u_n (x^{u_n} - x^{u_T^*}),$$

the first term converges by weak-\* convergence (since  $e^{-rt} c x^{u_T^*} \in L^1$ ) and the second to zero by strong  $L^1$  convergence, so  $J_T(u_n) \rightarrow J_T(u_T^*) = V_T^{BV}$ .  $\square$

*Proof of Proposition 6.10* A maximizing sequence  $L_n$  has, by  $BV(0, T) \hookrightarrow L^1(0, T)$ , a subsequence  $L_n \rightarrow L_T^* \in \mathcal{L}_{ad}$  in  $L^1$ , whence  $u_{L_n} \rightarrow u_{L_T^*}$  in  $L^1$ ; continuous dependence and boundedness give  $J_T(u_{L_n}) \rightarrow J_T(u_{L_T^*})$ .  $\square$

## E Proofs in Section 7

*Proof of Proposition 7.1* Write  $x^\varepsilon := x^{u^* + \varepsilon h}$ ,  $E^\varepsilon$  for its environment, and  $w^\varepsilon := (x^\varepsilon - x^*)/\varepsilon - z$  for the remainder we must show is  $o(1)$  in  $C([0, T]; L^1)$ . Continuous dependence (Proposition 4.9) gives the uniform difference-quotient bounds  $\|x^\varepsilon - x^*\|_{C([0, T]; L^1)} = O(\varepsilon)$  and  $\|E^\varepsilon - E^*\|_{C([0, T])} = O(\varepsilon)$ , so  $q^\varepsilon := (x^\varepsilon - x^*)/\varepsilon$  is bounded in  $C([0, T]; L^1)$  and  $\delta E^\varepsilon := (E^\varepsilon - E^*)/\varepsilon$  is bounded in  $C([0, T])$ , with  $|\delta E^\varepsilon| \leq \|\chi\|_\infty \|q^\varepsilon\|_{L^1}$ .

*Expansions.* By  $E \mapsto g(E, \cdot) \in C^1(\mathbb{R}_+; W^{1, \infty})$  and  $E \mapsto \mu(E, \cdot) \in C^1(\mathbb{R}_+; L^\infty)$ ,  
 $g(E^\varepsilon, \cdot) - g(E^*, \cdot) = \partial_E g(E^*, \cdot) (E^\varepsilon - E^*) + R_g^\varepsilon$ ,  $\mu(E^\varepsilon, \cdot) - \mu(E^*, \cdot) = \partial_E \mu(E^*, \cdot) (E^\varepsilon - E^*) + R_\mu^\varepsilon$ ,  
with  $\|R_g^\varepsilon\|_{W^{1, \infty}} + \|R_\mu^\varepsilon\|_{L^\infty} = o(\|E^\varepsilon - E^*\|_C) = o(\varepsilon)$ .

*Equation for the remainder.* Subtracting the transport equations for  $x^\varepsilon$  and  $x^*$ , dividing by  $\varepsilon$ , and subtracting the linearized equation (42), the remainder  $w^\varepsilon$  solves a transport equation with the same principal part as the linearization,

$$\partial_t w^\varepsilon + \partial_l (g(E^*, l) w^\varepsilon) + (\mu(E^*, l) + u^*) w^\varepsilon = \partial_l (\partial_E g(E^*, l) \delta E^\varepsilon (x^\varepsilon - x^*)) - \partial_E \mu \delta E^\varepsilon (x^\varepsilon - x^*) + \rho^\varepsilon,$$

where every term on the right is either (i) a product of a bounded factor with one of  $x^\varepsilon - x^* = O(\varepsilon)$  or  $\delta E^\varepsilon - \delta E$ , or (ii) a remainder  $\rho^\varepsilon$  collecting  $R_g^\varepsilon, R_\mu^\varepsilon$  tested against the bounded  $q^\varepsilon$ ; hence  $\|\rho^\varepsilon\|_{L^1} = o(1)$  and the quadratic products are  $O(\varepsilon)$ . The boundary trace is control-independent, so  $w^\varepsilon(t, l_0)$  satisfies the homogeneous version of (43) up to an  $o(1)$  term obtained by the same expansion of  $g(E^\varepsilon, l_0)$ , and  $w^\varepsilon(0, \cdot) = 0$ .

*Grönwall closure.* Testing this transport equation by  $\text{sgn}(w^\varepsilon)$  and integrating in  $l$  (the outflow trace at  $l_m$  has a sign that removes mass, and the inflow trace contributes the  $o(1)$  boundary term) gives

$$\frac{d}{dt} \|w^\varepsilon(t, \cdot)\|_{L^1} \leq C_T \|w^\varepsilon(t, \cdot)\|_{L^1} + \beta^\varepsilon(t), \quad \|\beta^\varepsilon\|_{L^1(0, T)} = o(1) + O(\varepsilon),$$

with  $C_T$  the uniform coefficient bound from (7)–(10) on  $[0, M_T]$  (the  $\partial_l(g \cdot)$  term contributes through  $\|\partial_l g\|_\infty$  exactly as in Proposition 4.9). Since  $w^\varepsilon(0, \cdot) = 0$ , Grönwall gives  $\|w^\varepsilon\|_{C([0, T]; L^1)} \leq e^{C_T T} \|\beta^\varepsilon\|_{L^1} \rightarrow 0$ . Thus  $q^\varepsilon \rightarrow z$  in  $C([0, T]; L^1)$ , which is the claim; uniqueness of  $z$  follows from the same Grönwall estimate applied to a difference of two solutions.  $\square$

*Proof of Lemma 7.3* From (45),

$$|\mathcal{G}_{x^*}[\lambda](t)| \leq \|\lambda(t, \cdot)\|_\infty \left[ \|\partial_E g\|_\infty |x^*(t, l_0^+)| + \|\partial_E g\|_\infty \text{TV}_\Omega(x^*(t, \cdot)) + (\|\partial_l \partial_E g\|_\infty + \|\partial_E \mu\|_\infty) \|x^*(t, \cdot)\|_{L^1} \right],$$

and the bracket is uniformly bounded by the state bounds and (41).  $\square$

*Proof of Proposition 7.7* Multiply (42) by  $\lambda_{pv}^* = e^{-rt} \lambda^*$ , integrate over  $(0, T) \times \Omega$ , and integrate by parts in  $t$  and  $l$ . The terminal, outflow, fixed-initial, and linearized-inflow conditions remove the boundary variations; the environmental-variation terms combine into  $\mathcal{G}_{x^*}[\lambda^*]$ , and (46) cancels every term in  $z$ , leaving  $\int_0^T e^{-rt} \int_\Omega x^*(c - \lambda^*) h$ .  $\square$

*Proof of Theorem 7.8* Convexity of  $U_{ad}^{BV}$  makes  $u_\varepsilon = u^* + \varepsilon(v - u^*)$  admissible for  $\varepsilon \in [0, 1]$ ; optimality gives  $J_T(u_\varepsilon) - J_T(u^*) \leq 0$ . Divide by  $\varepsilon$ , let  $\varepsilon \downarrow 0$ , and apply Proposition 7.7.  $\square$

*Proof of Theorem 7.9* Under (48), small one-sided BV bump directions into the box, supported in small neighborhoods, are feasible; localizing (47) gives  $x^* S^*(v - u^*) \leq 0$  for all  $v \in [0, u_{\max}]$  at a.e. Lebesgue point, equivalent to the stated arg-max; for  $x^* > 0$ , maximizing the affine map gives (49).  $\square$

## F Proofs in Section 8

*Proof of Lemma 8.5* Since  $\{S^* < 0\}$  is a lower set it equals  $[l_0, L_-)$  and  $\{S^* > 0\}$  is an upper set equal to  $(L_+, l_m]$ ; the ordered sign condition forbids a negative value above a positive one, so  $L_- \leq L_+$ , and on the open gap  $(L_-, L_+)$  the sign is neither  $< 0$  nor  $> 0$ , hence  $S^* = 0$  there, giving (51). If both sign sets are nonempty,  $L_-, L_+ \in (l_0, l_m)$  and continuity forces  $S^*(L_-) = S^*(L_+) = 0$  as limits of negative (resp. positive) values. If, say,  $\{S^* < 0\} = \emptyset$  then  $L_- = l_0$  by convention and no zero is forced at  $l_0$ ; symmetrically when  $\{S^* > 0\} = \emptyset$ . The converse is immediate.  $\square$

*Proof of Theorem 8.6* Lemma 8.5 gives the sign pattern in each case; combined with the bang–bang rule (49) (valid where  $x^* > 0$ ) it yields  $u^* = 0$  where  $S^* < 0$  and  $u^* = u_{\max}$  where  $S^* > 0$ . In cases (i)–(ii) one sign set is empty, so no interior threshold is forced and the conclusion holds off the zero set; in case (iii) both endpoints are interior zeros and the open interval  $(L_-, L_+)$  is the singular set.  $\square$

*Proof of Theorem 8.7* The cases are Definition 8.3 combined with (49).  $\square$

*Proof of Proposition 8.8* For  $a \in \Omega$ ,  $\{t : L_+(t) < a\} = \bigcup_{q \in \mathbb{Q}, l_0 < q < a} \{t : S^*(t, q) > 0\}$  is measurable since each  $S^*(\cdot, q)$  is; similarly for  $L_-$ .  $\square$

*Proof of Proposition 8.9* The implicit function theorem.  $\square$

*Proof Proof of Proposition 8.10* Strict increase gives at most one zero with the correct orientation. For the converse, with  $\theta(l) = (l - l_0)/(l_m - l_0)$  and  $A > 2$ , set  $S_A(l) := (\theta - \frac{1}{2})(1 + A\theta(1 - \theta))$ . Since  $1 + A\theta(1 - \theta) > 0$ ,  $\text{sgn } S_A = \text{sgn}(\theta - \frac{1}{2})$ , a unique upward crossing at  $L = (l_0 + l_m)/2$ ; yet  $dS_A/d\theta|_0 = 1 - A/2 < 0$ , so  $S_A$  is not increasing.  $\square$

*Proof of Proposition 8.11* The sign margins exclude exterior zeros; the slope bound makes  $S$  strictly increasing on the central interval, and the endpoint signs give one zero by the intermediate value theorem. The perturbation bounds preserve both.  $\square$

## G Proofs in Section 9

*Proof of Theorem 9.3* The difference  $\delta := \lambda - \lambda_{\text{red}}$  solves  $\bar{g}\delta' = a\delta - \chi\Gamma$ ,  $\delta(l_m) = 0$ , which by linearity and (59) equals  $\Gamma\psi$ . Applying  $\mathcal{G}^*$ ,  $\Gamma = \mathcal{G}^*[\lambda] = A + \Gamma B$ , so  $(1 - B)\Gamma = A$ ; under  $1 - B \neq 0$ ,  $\Gamma = A/(1 - B)$ . Substitution gives (62).  $\square$

*Proof of Lemma 9.5*  $A, B$  are linear in  $g_E, g'_E, \mu_E$ ; the uniform  $BV/L^1$  bounds on  $x^*$  and uniform bounds on  $\lambda_{\text{red}}, \psi$  give  $|A| + |B| \leq C\varepsilon$ ;  $|1 - B| \geq 1 - C\varepsilon$  closes the estimate.  $\square$

*Proof of Theorem 9.6*  $|\Gamma| \leq |A|/(1 - \beta)$ , so  $S' \geq \eta - \frac{|A|}{1 - \beta} \|\psi'\|_\infty > 0$ ; the endpoint signs give one crossing.  $\square$

*Proof of Theorem 9.7* The value bound gives  $S < 0$  on the left margin and  $S > 0$  on the right margin, so all zeros lie centrally; the slope bound gives  $S' > 0$  there; the opposite end signs give one crossing. This is Proposition 8.11 applied to  $S = S_{\text{red}} - \Gamma\psi$ .  $\square$

*Proof of Proposition 9.9*  $0 = S(L^*) = S_{\text{red}}(L^*) - \Gamma\psi(L^*)$ ; expanding about  $L_{\text{red}}$  with  $S_{\text{red}}(L_{\text{red}}) = 0$  and  $L^* - L_{\text{red}} = O(\Gamma)$  gives the claim.  $\square$

*Proof of Lemma 9.10* Since  $a/\bar{g} = r/\bar{g} + q$  with  $q = (\bar{\mu} + u)/\bar{g}$ , the integrating factor in (60) splits as  $\exp(-\int_\xi^s a/\bar{g}) = e^{-r\tau(\xi, s)} \exp(-\int_\xi^s q)$ . Using  $x^*(\xi) = \frac{p}{\bar{g}(\xi)} \exp(-\int_{l_0}^\xi q)$ ,

$$\bar{g}(\xi)\psi_r(\xi)x^*(\xi) = p e^{-\int_{l_0}^\xi q} \int_\xi^{l_m} \frac{\chi(s)}{\bar{g}(s)} e^{-r\tau(\xi, s)} e^{-\int_\xi^s q} ds = \int_\xi^{l_m} \chi(s) e^{-r\tau(\xi, s)} \underbrace{\frac{p}{\bar{g}(s)} e^{-\int_{l_0}^s q}}_{= x^*(s)} ds = W_r(\xi).$$

The forward survival  $l_0 \rightarrow \xi$  and backward survival  $\xi \rightarrow s$  telescope to  $l_0 \rightarrow s$ ; the identity uses only the closed forms and so holds for bang–bang  $u$ .  $\square$

*Proof of Theorem 9.11* Substitute  $\psi'_r = (a\psi_r - \chi)/\bar{g}$  into the smooth form (55):

$$g_E\psi'_r - \mu_E\psi_r = \left(\frac{g_E a}{\bar{g}} - \mu_E\right)\psi_r - \frac{g_E\chi}{\bar{g}}.$$

With  $a = r + \bar{\mu} + u$ , the algebraic identities  $\frac{g_E(\bar{\mu} + u)}{\bar{g}} - \mu_E = -\bar{g}b$  and  $-g_E/\bar{g} = \alpha$  give  $\frac{g_E a}{\bar{g}} - \mu_E = -\bar{g}b - r\alpha$  and  $-g_E\chi/\bar{g} = \alpha\chi$ , hence

$$g_E\psi'_r - \mu_E\psi_r = (-\bar{g}b - r\alpha)\psi_r + \alpha\chi.$$

Multiplying by  $x^*$  and integrating,

$$B(r) = - \int b(\bar{g}\psi_r x^*) - r \int \alpha\psi_r x^* + \int \alpha\chi x^*.$$

By Lemma 9.10,  $\bar{g}\psi_r x^* = W_r$  and  $\alpha\psi_r x^* = \frac{\alpha}{\bar{g}}W_r$ , giving (64). At  $r = 0$ ,  $W_0 = W_{E^*}$ , so  $B(0) = A(E - \int bW_{E^*}) = A - C = \Phi'(E^*)$  by (24).

For the limit, change variables from size  $s$  to travel time  $t = \tau(\xi, s)$ ,  $ds = \bar{g}(s) dt$ , in (63):

$$W_r(\xi) = \int_0^{\tau(\xi, l_m)} H_\xi(t) e^{-rt} dt, \quad H_\xi(t) := \chi(s(\xi, t)) x^*(s(\xi, t)) \bar{g}(s(\xi, t)),$$

where  $s(\xi, t)$  is the size reached from  $\xi$  after travel time  $t$ , so  $H_\xi(0) = \chi(\xi)x^*(\xi)\bar{g}(\xi)$ . Under the stated continuity,  $H_\xi$  is continuous at  $t = 0$  and uniformly bounded, so the approximate-identity (Abelian) estimate gives  $rW_r(\xi) \rightarrow H_\xi(0) = \chi(\xi)x^*(\xi)\bar{g}(\xi)$  as  $r \rightarrow \infty$ , with  $0 \leq rW_r(\xi) \leq \sup H_\xi < \infty$  uniformly in  $\xi$ . By dominated convergence,

$$r \int_{l_0}^{l_m} \frac{\alpha(\xi)}{\bar{g}(\xi)} W_r(\xi) d\xi \rightarrow \int_{l_0}^{l_m} \frac{\alpha(\xi)}{\bar{g}(\xi)} \chi(\xi)x^*(\xi)\bar{g}(\xi) d\xi = A(E),$$

while  $0 \leq W_r(\xi) \leq (\sup H_\xi)/r \rightarrow 0$  gives  $\int b W_r \rightarrow 0$ . Hence  $B(r) \rightarrow A(E) - 0 - A(E) = 0$ .  $\square$

*Proof of Corollary 9.12* (a) is Theorem 9.11 with  $\Phi'(E^*) < 0$  and continuity of  $r \mapsto B(r)$ . (b) follows from  $B(r) \leq A^* < 1$ .  $\square$

*Proof of Theorem 9.15* The first two conditions exclude exterior zeros; the derivative enclosure makes  $S$  strictly increasing on  $I_k$ ; the endpoint signs and the intermediate value theorem give one upward zero in  $I_k$ .  $\square$

*Proof of Proposition 9.17* The intermediate value theorem gives a zero in each of  $(q_1, q_2)$ ,  $(q_2, q_3)$ .  $\square$

## References

- [1] Metz, J.A., Diekmann, O.: The Dynamics of Physiologically Structured Populations. Springer (2014)
- [2] Diekmann, O., Gyllenberg, M., Metz, J.: Steady-state analysis of structured population models. Theoretical population biology **63**(4), 309–338 (2003)
- [3] Cai, J., Chen, X., Gu, L., Chen, J., Chu, N., Wang, L.S., Liang, Y., Yu, J.: Optimal harvesting for nonlinear size-structured populations with nonlocal environmental feedback. Mathematics (2026)
- [4] Gyllenberg, M.: Mathematical aspects of physiologically structured populations: the contributions of jaj metz. Journal of biological dynamics **1**(1), 3–44 (2007)
- [5] Diekmann, O., Scarabel, F.: Age-structured population dynamics. arXiv preprint arXiv:2506.03405 (2025)
- [6] Yu, J., Wang, L.S., Liang, Y.: Rigorous analysis of a nonlocal transport–renewal system for physiologically structured populations. Mathematical Methods in the Applied Sciences (2026)
- [7] Bouguima, S.M., Kada, K.A.: Analysis and control of physiologically structured models with nonlocal diffusion. Differential Equations & Applications **15**(1) (2023)

- [8] Chen, M., Yuan, R.: Maximum principle for the optimal harvesting problem of a size-stage-structured population model. *Discrete & Continuous Dynamical Systems-Series B* **27**(8) (2022)
- [9] Webb, G.F.: *Theory of Nonlinear Age-dependent Population Dynamics*. CRC Press (1985)
- [10] Iannelli, M., Milner, F., et al.: *The basic approach to age-structured population dynamics*
- [11] Cushing, J.: Structured population dynamics. In: *Frontiers in Mathematical Biology*, pp. 280–295. Springer (1994)
- [12] Thieme, H.R.: *Mathematics in Population Biology*. Princeton University Press (2018)
- [13] Wang, L.S., Yu, J.: Analysis framework for stochastic predator–prey model with demographic noise. *Results in Applied Mathematics* **27**, 100621 (2025)
- [14] Diekmann, O., Gyllenberg, M., Metz, J., Thieme, H.R.: On the formulation and analysis of general deterministic structured population models i. linear theory: I. linear theory. *Journal of Mathematical Biology* **36**(4), 349–388 (1998)
- [15] Diekmann, O., Gyllenberg, M., Huang, H., Kirkilionis, M., Metz, J., Thieme, H.R.: On the formulation and analysis of general deterministic structured population models ii. nonlinear theory: II. nonlinear theory. *Journal of mathematical biology* **43**(2), 157–189 (2001)
- [16] Wang, L.S., Yu, J., Li, S., Liu, Z.: Analysis and mean-field limit of a hybrid PDE-ABM modeling angiogenesis-regulated resistance evolution. *Mathematics* **13**(17), 2898 (2025)
- [17] Beverton, R.J., Holt, S.J.: *On the Dynamics of Exploited Fish Populations* vol. 11. Springer (2012)
- [18] Clark, C.W.: *Mathematical Bioeconomics: the Mathematics of Conservation*. John Wiley & Sons (2010)
- [19] Opmeer, M.: Optimal harvesting of a continuously age-structured population with density dependence. *Plos one* **20**(9), 0333087 (2025)
- [20] Gurtin, M.E., Murphy, L.F.: On the optimal harvesting of age-structured populations: some simple models. *Mathematical Biosciences* **55**(1-2), 115–136 (1981)
- [21] Murphy, L.F., Smith, S.J.: Optimal harvesting of an age-structured population. *Journal of Mathematical Biology* **29**(1), 77–90 (1990)

- [22] Liu, Z., Wang, L.S., Yu, J., Zhang, J., Martel, E., Li, S.: Bidirectional endothelial feedback drives turing-vascular patterning and drug-resistance niches: a hybrid PDE-agent-based study. *Bioengineering* **12**(10), 1097 (2025)
- [23] Brokate, M.: Pontryagin’s principle for control problems in age-dependent population dynamics. *Journal of Mathematical Biology* **23**(1), 75–101 (1985)
- [24] Anita, S.: *Analysis and Control of Age-dependent Population Dynamics* vol. 11. Springer (2013)
- [25] Barbu, V., Iannelli, M.: Optimal control of population dynamics. *Journal of optimization theory and applications* **102**(1), 1–14 (1999)
- [26] Feichtinger, G., Tragler, G., Veliov, V.M.: Optimality conditions for age-structured control systems. *Journal of Mathematical Analysis and Applications* **288**(1), 47–68 (2003)
- [27] Pontryagin, L.S.: *Mathematical Theory of Optimal Processes*. Routledge (2018)
- [28] Kato, N.: Maximum principle for optimal harvesting in linear size-structured population. *Mathematical Population Studies* **15**(2), 123–136 (2008)
- [29] Kato, N.: Optimal harvesting for nonlinear size-structured population dynamics. *Journal of Mathematical Analysis and Applications* **342**(2), 1388–1398 (2008)
- [30] Hritonenko, N., Yatsenko, Y., Goetz, R.-U., Xabadia, A.: A bang–bang regime in optimal harvesting of size-structured populations. *Nonlinear Analysis: Theory, Methods & Applications* **71**(12), 2331–2336 (2009)
- [31] Davydov, A., Platov, A.: Optimization of stationary solution of a model of size-structured population exploitation. *Journal of Mathematical Sciences* **176**(6), 860–869 (2011)
- [32] Anita, S., Mosneagu, A.-M.: Optimal harvesting for age-structured population dynamics with size-dependent control. *Mathematical Control and Related Fields* **9**, 607–621 (2019)
- [33] Anița, S., Moșneagu, A.-M.: Optimal harvesting for size-dependent control. *Vietnam Journal of Mathematics* **47**(4), 881–895 (2019)
- [34] Liang, Y., Wang, L.S., Yu, J., Liu, Z.: Global well-posedness and stability of nonlocal damage-structured lineage model with feedback and dedifferentiation. *Mathematics* **13**(22), 3583 (2025)
- [35] Hritonenko, N., Yatsenko, Y.: Bang-bang, impulse, and sustainable harvesting in age-structured populations. *Journal of Biological Systems* **20**(02), 133–153 (2012)
- [36] Coclite, G.M., Garavello, M.: A time-dependent optimal harvesting problem with

- measure-valued solutions. *SIAM Journal on Control and Optimization* **55**(2), 913–935 (2017)
- [37] Calsina, À., Saldaña, J.: A model of physiologically structured population dynamics with a nonlinear individual growth rate. *Journal of Mathematical Biology* **33**(4), 335–364 (1995)
- [38] Wang, L.S., Yu, J., Liu, Z.: A damage-structured PDE model of stem cell hierarchies: The dual role of dedifferentiation in tissue homeostasis and aging. *Plos one* **21**(2), 0335163 (2026)
- [39] Bressan, A., Coclite, G.M., Shen, W.: A multidimensional optimal-harvesting problem with measure-valued solutions. *SIAM Journal on Control and Optimization* **51**(2), 1186–1202 (2013)
- [40] Yu, J., Wang, L.S., Liu, Z., Liu, J.: Pattern suppression and recovery under one-way versus two-way chemotactic coupling in hybrid partial differential equation–ordinary differential equation models. *Transport Phenomena* (0) (2026)
- [41] Carrillo, J.A., Colombo, R.M., Gwiazda, P., Ulikowska, A.: Structured populations, cell growth and measure valued balance laws. *Journal of Differential Equations* **252**(4), 3245–3277 (2012)
- [42] Debiec, T., Doumic, M., Gwiazda, P., Wiedemann, E.: Relative entropy method for measure solutions of the growth-fragmentation equation. *SIAM Journal on Mathematical Analysis* **50**(6), 5811–5824 (2018)
- [43] Wang, L.S., Yu, J.: Algebraic–spectral thresholds and discrete–continuous stability transfer in Leslie–Gower systems. *Electronic Research Archive* **34**(1), 251–290 (2026)
- [44] Kakumani, B.K., Tumuluri, S.K.: Optimal harvesting control for a nonlinear mckendrick–von foerster equation with generic cost functional. *Mathematical Control and Related Fields*, 0–0 (2026)
- [45] Freiburger, M., Kuhn, M., Prskawetz, A., Sanchez-Romero, M., Wrzaczek, S.: Optimization in age-structured dynamic economic models. In: *The Unaffordable Price of Static Decision-Making Models: Challenges in Economics and Management Science*, pp. 35–62. Springer (2025)
- [46] Kang, Y., Nie, L.: Dynamical analysis and optimal control of an age-structured epidemic model with asymptomatic infection and multiple transmission pathways. *Mathematical Methods in the Applied Sciences* **47**(12), 9669–9702 (2024)
- [47] Khan, A., Zaman, G.: Optimal control strategies for an age-structured seir epidemic model. *Mathematical Methods in the Applied Sciences* **45**(14), 8701–8717 (2022)

- [48] Wu, P., Ruan, S.: An age-structured syphilis model, ii: optimal control and numerical simulation. In: Proceedings A, vol. 481, p. 20230809 (2025). The Royal Society
- [49] Chen, Z., Feng, H.: Numerical dynamics and optimal control for multi-strain age-structured epidemic model. *Journal of Mathematical Biology* **90**(2), 17 (2025)
- [50] Wang, S.-F., Nie, L.-F.: Global dynamics and optimal control of multi-age structured vector disease model with vaccination, relapse and general incidence. *Qualitative theory of dynamical systems* **22**(1), 24 (2023)
- [51] Perthame, B.: *Transport Equations in Biology*. Springer (2007)
- [52] Ingram, W., Grace, M., Lombardi-Carlson, L., Henwood, T.: Catch rates, distribution and size/age composition of red grouper, *epinephelus morio*, collected during noaa fisheries bottom longline surveys from the us gulf of mexico. SEDAR12-DW05. Sustainable Fisheries Division, Miami, FL (2006)
- [53] Wang, L.S., Yu, J., Liang, Y., Zhang, J.: The breakdown of linear quasi-cycles: Demographic noise and absorbing boundaries in finite predator-prey systems. *Electronic Research Archive* **34**(6), 4248–4289 (2026)
- [54] Gwiazda, P., Marciniak-Czochra, A.: Structured population equations in metric spaces. *Journal of Hyperbolic Differential Equations* **7**(04), 733–773 (2010)
- [55] Düll, C., Gwiazda, P., Marciniak-Czochra, A., Skrzeczkowski, J.: *Spaces of Measures and Their Applications to Structured Population Models* vol. 36. Cambridge University Press (2021)
- [56] Yu, J., Wang, L.S.: Beyond diagonal noise: A better predator-prey modeling framework with cross-covariance. *PLoS One* **21**(5), 0350127 (2026)
- [57] Hritonenko, N., Kato, N., Yatsenko, Y.: Existence of measure-valued solutions in optimal control of age-structured populations. *Applicable Analysis* **102**(5), 1281–1293 (2023)
- [58] Wang, Z., Wang, D., Yu, J.: Multi-strategy hybrid improved intelligent algorithm for solving UAV-MTSP. *Information Technology and Control* **54**(2), 413–438 (2025)
- [59] Yu, J., Wang, L.S., Ban, S., Liang, Y.: From microscopic damage to macroscopic games: a dimensionality reduction of stem cell homeostasis. *Transport Phenomena* **1**(2), 20260037 (2026)
- [60] Gao, Y., Li, L., Yu, J.: Rolling prediction model of closing price based on EEMD data noise reduction and HGS-DELM. In: 2022 International Conference on Data Analytics, Computing and Artificial Intelligence (ICDACAI), pp. 255–260 (2022). IEEE

- [61] Sherman, J., Morrison, W.J.: Adjustment of an inverse matrix corresponding to a change in one element of a given matrix. *The Annals of Mathematical Statistics* **21**(1), 124–127 (1950)
- [62] Von Bertalanffy, L.: A quantitative theory of organic growth (inquiries on growth laws. ii). *Human biology* **10**(2), 181–213 (1938)
- [63] De Roos, A.M., Schellekens, T., Van Kooten, T., Van De Wolfshaar, K., Claessen, D., Persson, L.: Simplifying a physiologically structured population model to a stage-structured biomass model. *Theoretical population biology* **73**(1), 47–62 (2008)